NUREG/CR-3386
EGG-2260
Distribution Category: R2

DETECTION OF INADEQUATE CORE COOLING WITH CORE EXIT THERMOCOUPLES: LOFT PWR EXPERIENCE

James P. Adams
Glenn E. McCreery

Published November 1983

EG&G Idaho, Inc.
Idaho Falls, Idaho 83415

Prepared for the
U.S. Nuclear Regulatory Commission
Washington, D.C. 20555
Under DOE Contract No. DE-AC07-76IDO1570
FIN No. A6048

ABSTRACT

Results from four previously reported loss-of-coolant accident simulations in the Loss of Fluid Test Facility at the Idaho National Engineering Laboratory are analyzed to determine the response of the core exit thermocouples to core cladding heatup resulting from core uncovery. A detailed analysis is presented for the reactor vessel thermal and hydraulic conditions existing during the core uncovery phase of the one experiment in which core exit thermocouples did not respond to the core uncovery. Conclusions are drawn regarding the limitations of the use of core exit thermocouples in measuring core uncovery and subsequent core heatup.

FIN No. A6048—LOFT Experimental Program

NRC FORM 335 (11-81)

U.S. NUCLEAR REGULATORY COMMISSION

BIBLIOGRAPHIC DATA SHEET

1. REPORT NUMBER *(Assigned by DDC)*
NUREG/CR-3386
EGG-2260

4. TITLE AND SUBTITLE
Detection of Inadequate Core Cooling with Core Exit Thermocouples: LOFT PWR Experience

2. *(Leave blank)*

3. RECIPIENT'S ACCESSION NO.

7. AUTHOR(S)
J. P. Adams, G. E. McCreery

5. DATE REPORT COMPLETED
MONTH November YEAR 1983

9. PERFORMING ORGANIZATION NAME AND MAILING ADDRESS *(Include Zip Code)*
EG&G Idaho, Inc.
Idaho Falls, ID 83415

DATE REPORT ISSUED
MONTH November YEAR 1983

6. *(Leave blank)*

8. *(Leave blank)*

12. SPONSORING ORGANIZATION NAME AND MAILING ADDRESS *(Include Zip Code)*
Division of Nuclear Regulatory Research
Office of Accident Evaluation
U.S. Nuclear Regulatory Commission
Washington, DC 20555

10. PROJECT/TASK/WORK UNIT NO.

11. FIN NO.

13. TYPE OF REPORT

PERIOD COVERED *(Inclusive dates)*

15. SUPPLEMENTARY NOTES

14. *(Leave blank)*

16. ABSTRACT *(200 words or less)*

Results from four previously reported loss-of-coolant accident simulations in the Loss of Fluid Test Facility at the Idaho National Engineering Laboratory are analyzed to determine the response of the core exit thermocouples to core cladding heatup resulting from core uncovery. A detailed analysis is presented for the reactor vessel thermal and hydraulic conditions existing during the core uncovery phase of the one experiment in which core exit thermocouples did not respond to the core uncovery. Conclusions are drawn regarding the limitations of the use of core exit thermocouples in measuring core uncovery and subsequent core heatup.

17. KEY WORDS AND DOCUMENT ANALYSIS

17a. DESCRIPTORS

17b. IDENTIFIERS/OPEN-ENDED TERMS

18. AVAILABILITY STATEMENT
Unlimited

19. SECURITY CLASS *(This report)*
Unclassified

21. NO. OF PAGES

20. SECURITY CLASS *(This page)*
Unclassified

22. PRICE
$

SUMMARY

The nuclear industry has recommended the use of core exit fluid thermocouples (TCs) to monitor the core uncovery and cladding thermal excursion that might occur as a result of a loss of coolant accident (LOCA). The core exit TCs would monitor the cladding thermal excursion by detecting superheated steam as it exited the core.

Data taken during four LOCA simulations in the Loss of Fluid Test (LOFT) Facility have been analyzed to determine the limitations inherent in using core exit TCs in this way. The experiments analyzed were

1. *Experiment L2-5*—a large-break LOCA simulation in which the core was allowed to uncover subsequent to completion of the blowdown—refill—reflood phase

2. *Experiment L3-6/L8-1*—a 4-in. small-break LOCA simulation with delayed pump trip

3. *Experiment L5-1*—a 14-in. intermediate-break LOCA simulation with low-head accumulator injection

4. *Experiment L8-2*—a 14-in. intermediate-break LOCA simulation with delayed accumulator injection.

In the LOFT facility, the core exit TCs are Type K chromel—alumel TCs mounted in cutouts in the fuel assembly upper grid plates and are located 1 in. above the top of the fuel rods. This arrangement results in a TC that is expected to be at least as responsive to core uncovery as the core exit TCs in a typical commercial pressurized water reactor (PWR).

Two general limitations have been identified regarding the ability of core exit fluid TCs to monitor a core uncovery. First, there is a delay between the core uncovery and the TC response. This delay ranged from 28 to 182 s in the four LOCA simulations, and could have been even longer in one case had the reactor operators not initiated core reflood. The delay is judged to be caused by a film of water that coats the TC and must be removed before the TC can respond to the vapor superheat. The film of water is caused by continuing drainage in the upper plenum.

Second, the measured core exit TC response was several hundred Kelvin lower than the maximum cladding temperatures in the core. This temperature difference results from the vapor superheat at the core exit being limited by the cladding temperatures near the core exit in the LOFT experiments. These cladding temperatures were up to 360 K (648°F) lower than those in the high-power regions near the core center.

In conclusion, any procedure that relies on the response of core exit fluid TCs to monitor a core uncovery should take these two limitations into account. There may be accident scenarios in which these TCs would not detect inadequate core cooling that preceded core damage.

ACKNOWLEDGMENTS

We would like to acknowledge, with thanks, the following individuals who have contributed to the understanding of the phenomena and to the production of this report. Without their assistance, this report could not have been completed in its present form. In alphabetical order: D. Batt, V. Berta, D. Croucher, D. Hansen, and S. Naff for helpful discussions and technical input; P. Knecht for editorial review; and D. Johnson for producing the computer plots of data.

CONTENTS

NOMENCLATURE

Symbol	Definition	Units
α	Vapor fraction	—
a	Interfacial area formed per unit time	$m^2/(s \cdot rod)$, $ft^2/(s \cdot rod)$
$\bar{A}$	Time averaged surface area in froth	m^2, ft^2
A_R	Fuel rod surface area	m^2, ft^2
A_x	Cross-sectional flow area per fuel rod	m^2, ft^2
C_o	Distribution parameter	—
C_E	Droplet concentration	kg/m^3, lbm/ft^3
d	Outer diameter	m, ft
d	Drop diameter	m, ft
g	Gravitational constant	9.8 m/s^2, 32 ft/s^2
g_c	Dimensional constant	32.17 $lbm \cdot ft/(lbf \cdot s^2)$
h_{fg}	Specific enthalpy of vaporization	kJ/kg, Btu/lbm
$j_{g,f}$	Volumetric flux for vapor, liquid	m/s, ft/s
K_d	Deposition coefficient	m/s, ft/s
$K_{g,f}$	Kudateladze number for vapor, liquid	—
μ	Viscosity	$N \cdot s/m^2$, $lbf \cdot s/ft^2$
M	Mass	kg, lbm
$\dot{M}$	Mass flow rate	kg/s, lbm/s
ϱ	Density	kg/m^3, lbm/ft^3
P	Power	kW
$\bar{q}$	Time averaged heat flux	kW/m^2, $Btu/(h \cdot ft^2)$
$(q/A)_{CHF\ (Zuber)}$	CHF correlation by Zuber	kW/m^2, kW/ft^2
$(q/A)_{rod\ max}$	Maximum heat flux from single fuel rod	kW/m^2, kW/ft^2
r_d	Droplet radius	m, ft
σ	Surface tension	N/m, lbf/ft

Symbol	Definition	Units
T	Temperature	K, °F
V_g	Velocity	m/s, ft/s
Y_c	Collapsed level	m, ft
Y_s	Froth level	m, ft
V_{gj}	Drift flux	m/s, ft/s
ΔT	Temperature differential	K, °F
x	Quality	—
Subscripts		
o	Initial condition	
BLCL	Broken-loop cold leg	
BLHL	Broken-loop hot leg	
DC	Downcomer	
ECCS	Emergency core cooling system	
f	Liquid	
g	Vapor	
ILCL	Intact-loop cold leg	
ILHL	Intact-loop hot leg	
out core	Exiting core	
out DC	Exiting downcomer	
RV	Reactor vessel	
sat	Saturation	
t	Terminal	
x	Cross section	

THERMOCOUPLE DESIGNATORS

Typical fuel rod cladding thermocouple designators are obtained from the corresponding fuel rod positions and elevations shown in the following figure. For example, in the designator TE-5F08-026, 5 = fuel assembly number; F = fuel assembly column; 08 = fuel assembly row; 026 = transducer elevation, inches above bottom of fuel rod.

In the typical core exit thermocouple designator TE-5UP-4, 5 = fuel assembly number and 4 = core exit thermocouple number for that fuel assembly.

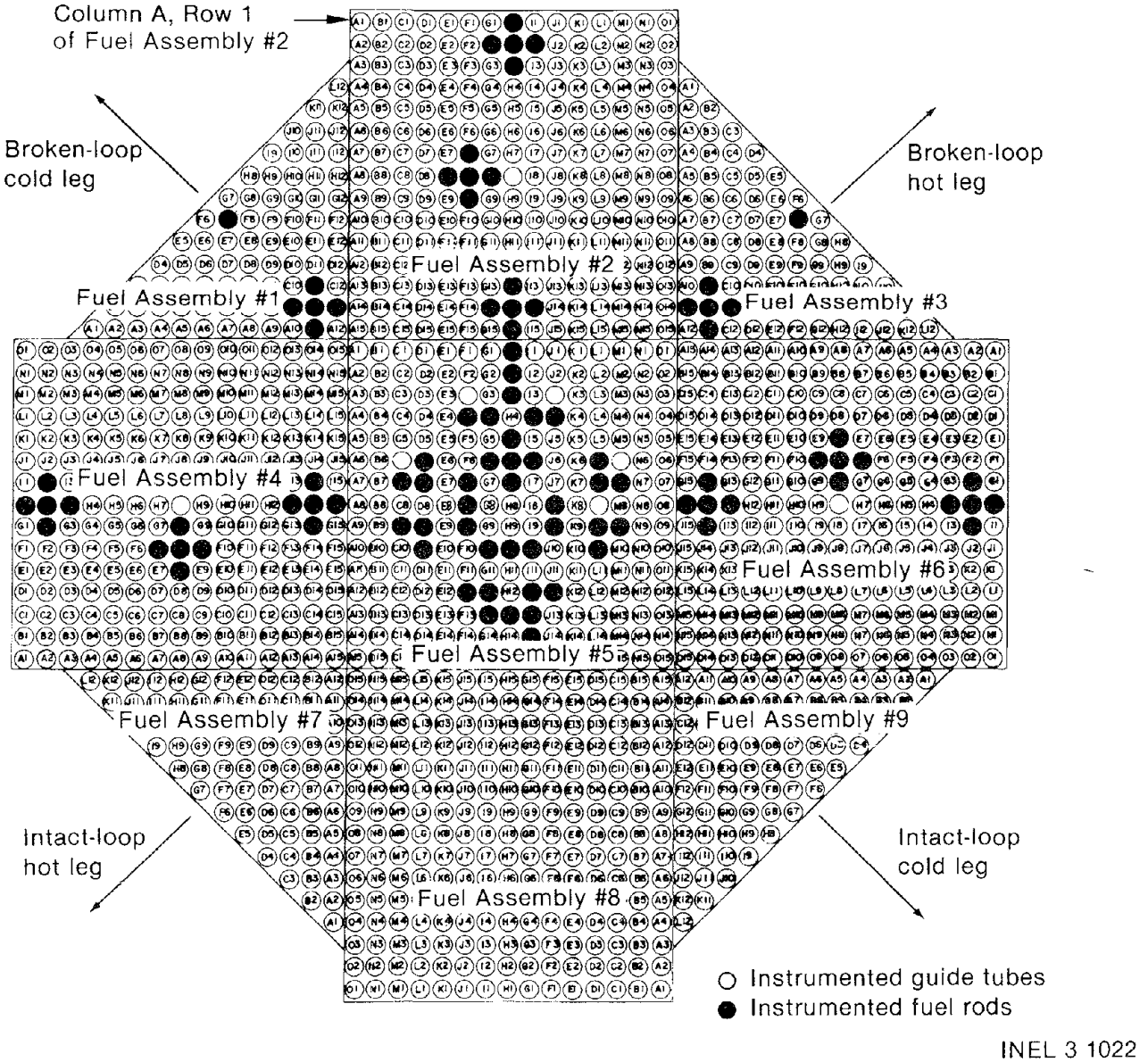

INEL 3 1022

DETECTION OF INADEQUATE CORE COOLING WITH CORE EXIT THERMOCOUPLES: LOFT PWR EXPERIENCE

INTRODUCTION

This report examines the ability of core exit thermocouples (TCs) to respond to a core uncovery and heatup in the experimental pressurized water reactor (PWR) at the Loss of Fluid Test (LOFT) Facility at the Idaho National Engineering Laboratory (INEL). The results can be used to assess the ability of upper-plenum TCs to detect inadequate core cooling in a commercial PWR.

The fuel cladding in an inadequately cooled PWR core could, if this condition were not mitigated, exceed the 10CFR50 Appendix K cladding temperature limit of 1475 K (2200°F) with resultant fuel rod damage.[1] As a direct result of the March 1979 accident at the Three Mile Island Unit-2 PWR, the Nuclear Regulatory Commission (NRC) assessed the adequacy of existing PWR instrumentation for a wide range of off-nominal transients, including those that result in inadequate core cooling (ICC).[2] It was suggested, among other methods, that the TCs currently installed at the flow exit of a PWR core could be used to detect ICC. This use of the core exit TCs has been assumed in NRC Regulatory Guide 1.97, in which these TCs are considered Type C, Category 1 instruments.[3] PWR vendors have responded to this guideline by proposing ICC instrumentation and procedure packages that include the use of core exit TCs as a principal means to detect the ICC condition.[4]

The basis for the use of the core exit TCs to detect ICC is contained in the definition of ICC. The NRC staff has stated ". . . the core [is considered] to be in a state of ICC whenever the two-phase froth level falls below the top of the core and the core heatup is well in excess of conditions that have been predicted for calculated small break scenarios for which some uncovery with successful recovery from the accident have been predicted."[5] Since the NRC ICC definition implies an uncontrolled core uncovery in the reactor vessel—a condition that did not exist during the controlled experiments discussed in this report—the following working definition is used in this report: the approach to ICC shall be denoted by the occurrence of a boiling transition, in part or all of the core, coincident with a continually decreasing water level.

A boiling transition is indicated when the cladding temperature significantly exceeds the saturation temperature, in response to a deficiency in the removal of decay heat from the core. As the cladding heats up in response to the inadequate cooling, the vapor surrounding the fuel rods superheats and the vapor flows out of the core. The vapor superheat is, in theory, detected by the core exit TCs. The message that an ICC condition (cladding heatup) exists in the core is transmitted by the vapor as superheat to the measurement station (TC location) outside the core.

For the indication of ICC (or approach to ICC) by core exit TCs to be adequate, the TCs must reliably, and in a timely manner, sense vapor superheat so the operator can reliably deduce the condition of the core from the TC response. These assumptions of reliability and timeliness are examined in this report, using data collected from LOFT experiments.

Several LOFT simulations of loss-of-coolant accidents (LOCAs) have been conducted during which the nuclear core was uncovered and allowed to heat up prior to being quenched. The results of one of these simulations, Experiment L2-5, raised the question of the reliability of core exit TC response as an indicator of ICC. To further address this question, the results of three other LOFT Experiments (L3-5/L8-1, L5-1, and L8-2) were reanalyzed with respect to ICC and core exit TC response. This report discusses the results of these four LOFT experiments in which the core uncovery scenario approached that expected during a small-break LOCA in a PWR: i.e., the uncoveries did not occur until a substantial time after reactor scram so that the thermal energy initially stored in the core had been dissipated, and the rate of uncovery was slow. The discussion is confined to the results that are pertinent to ICC and the resulting core exit TC responses.

LOFT FACILITY AND THERMOCOUPLE DESCRIPTION

The LOFT Facility includes a 55-MW(t) PWR with a complete primary system and a secondary system that includes an air cooled condenser for heat rejection. The LOFT PWR was volumetrically scaled to a commercial PWR and was designed to reproduce, both in time and in approximate magnitude, the phenomena expected to occur in a commercial PWR during off-nominal transients such as a LOCA. Reference 6 describes the LOFT Facility in detail and Reference 7 describes the LOFT scaling. Figure 1 shows the LOFT primary system. The reactor vessel and internals are shown in a cutaway view in Figure 2.

Commercial-PWR core exit TCs are mounted in a variety of ways. Some are housed in guide tubes and some are in the fluid stream. In general, the sensitive ends are oriented either vertically downward or horizontally and are located up to several inches above the top of the fuel rods. The leads are routed down and out through the reactor vessel bottom. In LOFT, the core exit TCs are mounted horizontally, ~1 in. above the top of the core, in cutouts in the fuel assembly upper grid plates (Figure 2), and the TC leads are routed out through the top of the reactor vessel. The TC mounting is shown in Figure 3, for a typical LOFT fuel assembly upper grid plate. The distribution pattern of the core exit TCs is shown in Figure 4.

Since the LOFT TCs are positioned within 1 in. of the top of the fuel rods and are in the normal fluid flow, it is expected that they will respond rapidly to superheated vapor exiting the core. Compared with commercial-PWR TCs that are mounted several inches above the fuel rods, and given similar

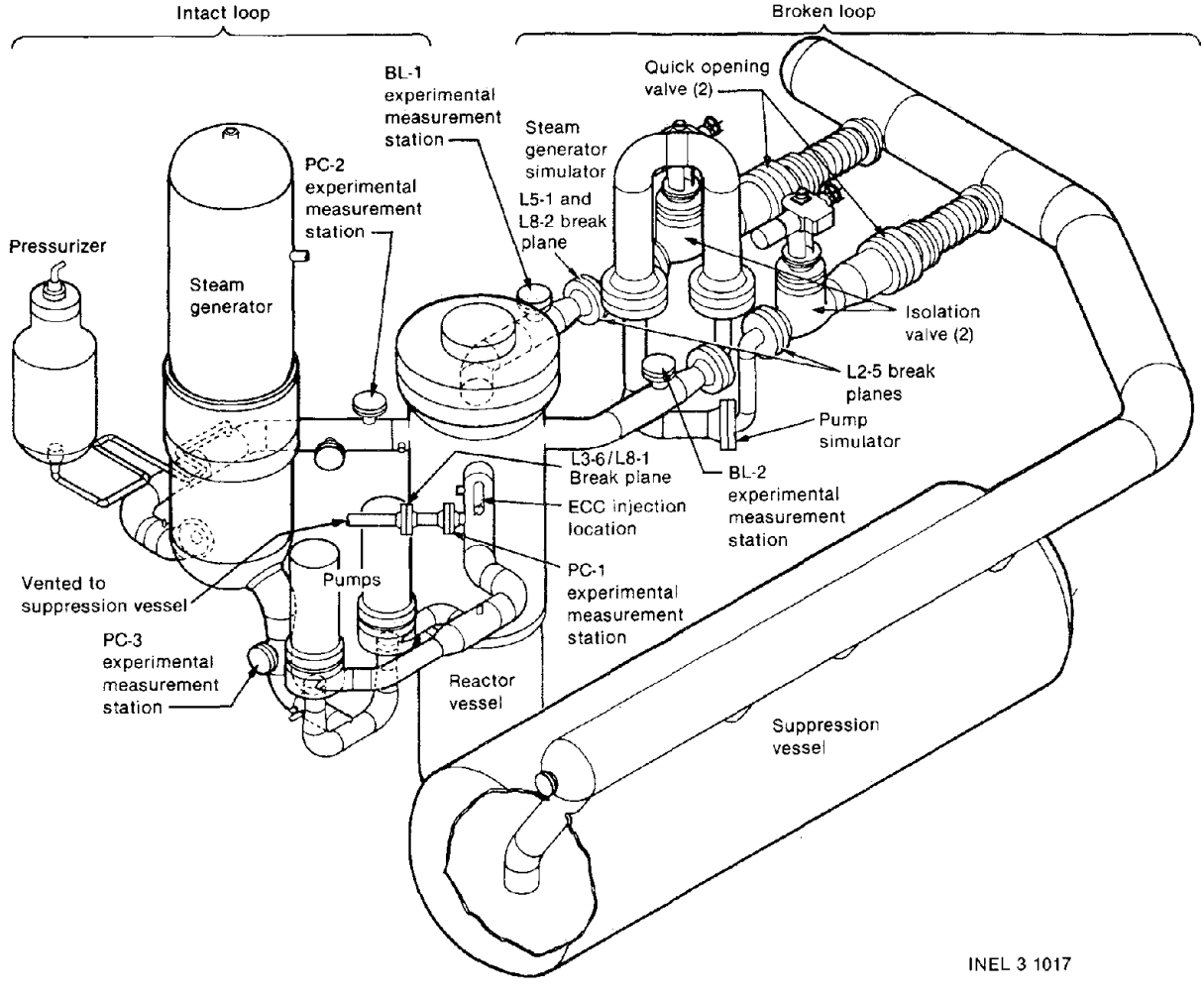

Figure 1. Axonometric schematic of the LOFT system.

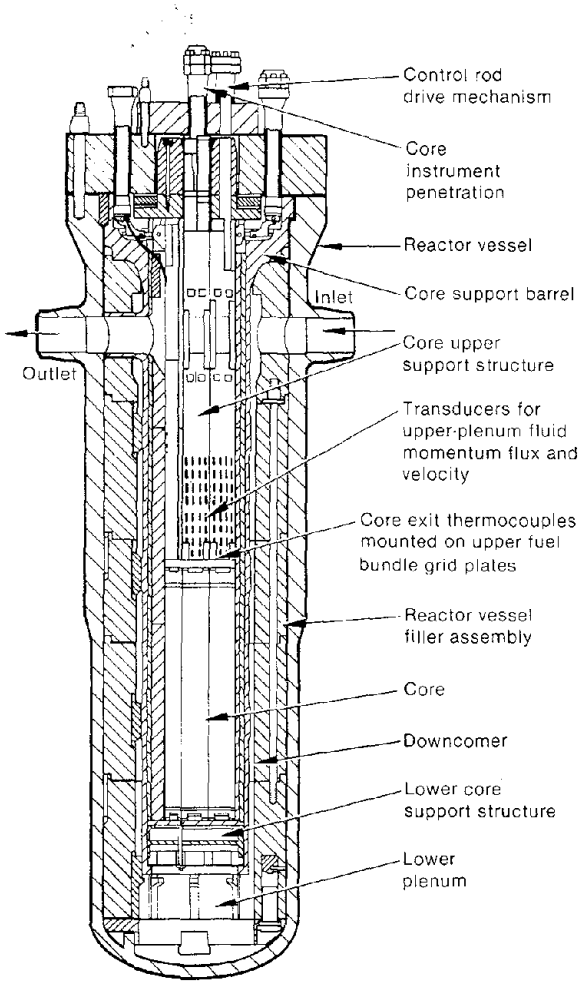

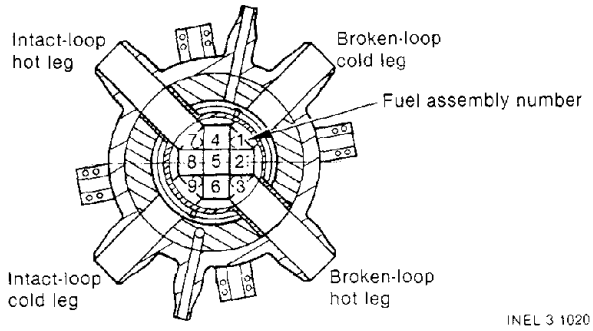

Figure 2. LOFT reactor vessel and internals.

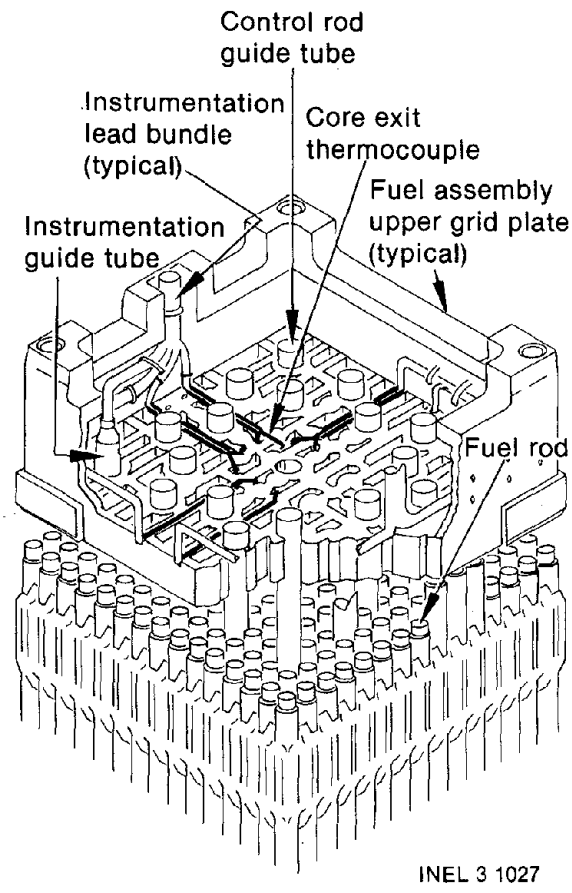

Figure 3. Mounting of LOFT core exit thermocouples on fuel bundle upper grid plate.

reactor vessel thermal-hydraulic conditions, the LOFT core exit TCs will be at least as responsive, and in many cases much more responsive, to core uncoveries.

The LOFT core exit TCs and cladding TCs are Type K chromel—alumel TCs with a normal high-temperature limit of 1645 K (2502°F), and are manufactured by SEMCO Instruments, Inc. They are insulated with either magnesia or alumina. The cladding TCs are sheathed with a titanium material and are calibrated up to 1580 K (2385°F), with a reference junction temperature of 339 K (151°F). The cladding TCs are a spade junction design and are laser welded to the fuel rod cladding. To avoid distortion of the fuel rod/TC assembly (due to differences in thermal expansion between the cladding and TC), dummy TC wires are welded at symmetric locations around the fuel rod. The core exit TCs, which measure fluid temperatures, are a grounded weld junction design and are sheathed with stainless steel. The core exit TCs are calibrated up to 1310 K (1899°F), with a reference junction temperature of 339 K (151°F). Both types of TC have a measured accuracy of 4.2% of reading plus 0.13% of range. For the core exit TCs, the frequency response is 3 Hz, which results in a 10% to 90% rise time of 0.12 s in response to an imposed step change in temperature. The frequency response and corresponding rise time for the cladding TCs are 4 Hz and 0.09 s. For both types of TC, the sensitivity at the reference temperature is 41.4 μV/K (23.0 μV/°F).

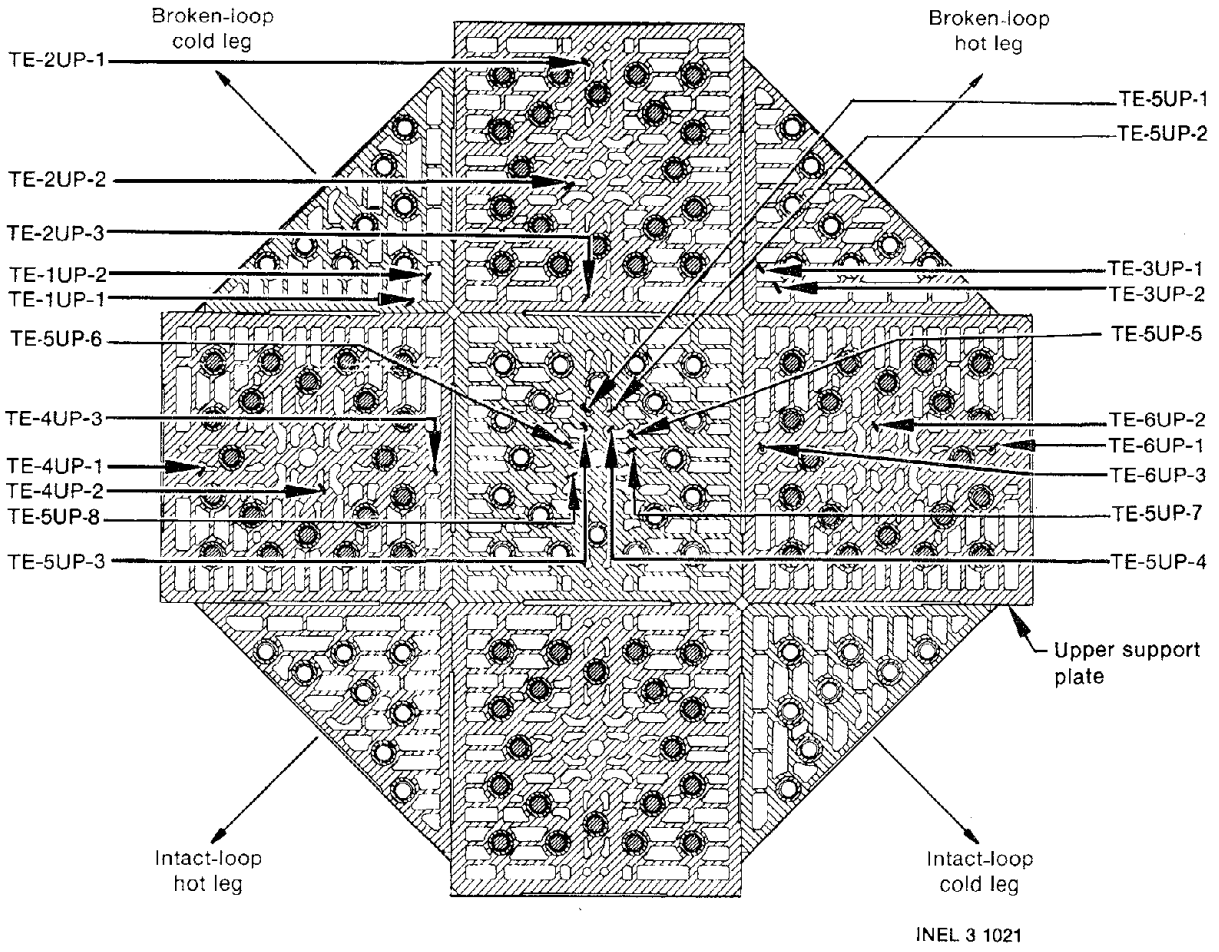

Figure 4. LOFT core exit thermocouple positions on fuel bundle upper grid plates.

EXPERIMENT RESULTS

The four LOFT experiments analyzed were Experiments L2-5 (a large-break LOCA simulation with a second core uncovery during the recovery phase),[8,9] L3-6/L8-1 (a pumps-on, small-break LOCA simulation),[10,11] and L5-1 and L8-2 (independent, intermediate-break LOCA simulations).[12,13] Table 1 describes these experiments. Table 2 lists the initial conditions and Table 3 gives the sequence of significant events for each experiment. More detailed descriptions are in the cited references.

Experiment L2-5

LOFT Experiment L2-5 (References 8 and 9) was initiated from conditions representative of full-power PWR operation, as noted in Table 2. The experiment was initiated by opening both quick-opening blowdown valves in the broken loop and allowing normal reactor protection systems to initiate automatically. The primary coolant pumps were stopped coincident with scram, as noted in Table 3. At the conclusion of the initial blowdown—refill transient, all emergency core cooling system (ECCS) injection was stopped, in accordance with the experiment plan, to test a recovery method for a subsequent experiment. A detailed analysis of the reactor vessel thermal-hydraulic conditions that existed during the resulting second heatup in Experiment L2-5 is included in the Appendix.

On loss of the ECCS injection, water inventory in the reactor vessel was reduced by a combination of boiling (due to decay heat) and carry-over out the loops (due to frothing) until the froth level decreased to the top of the core at 190 s. At this

Table 1. Description of LOFT Experiments L2-5, L3-6/L8-1, L5-1, and L8-2

Experiment	Date	Description
L2-5	6/16/82	Large cold-leg break experiment; normal ECCS; pumps stopped at initiation; multiple core uncovering including a. complete core uncovery at initiation and lasting 65 s; maximum cladding temperature 1077 K (1479°F) b. slow, complete core uncovery starting at 190 s and lasting 240 s; maximum cladding temperature 950 K (1251°F).
L3-6/L8-1	12/10/80	Scaled 4-in. intact-loop cold-leg break experiment (noncommunicative) with pumps running until 2371 s; complete core uncovery starting at 2395 s and lasting 78 s; ECCS delayed until after core uncovery; maximum cladding temperature 637 K (687°F).
L5-1	9/24/81	Scaled 14-in. broken-loop cold-leg break experiment (noncommunicative; accumulator pressure 1.66 MPa; slow 95% core uncovery starting at 108 s and lasting for 106 s; maximum cladding temperature 715 K (828°F).
L8-2	10/12/81	Scaled 14-in. broken-loop cold-leg break experiment (noncommunicative); ECCS delayed until after complete core uncovery; slow, complete core uncovery starting at 112 s and lasting for 194 s; maximum cladding temperature 987 K (1317°F). Primary coolant pumps restarted during core uncovery.

Table 2. Selected measured initial conditions for LOFT Experiments L2-5, L3-6/L8-1, L5-1, and L8-2

Parameter	L2-5	L3-6/L8-1	L5-1	L8-2
Hot-leg pressure (MPa)	14.94 ± 0.06	14.87 ± 0.14	14.83 ± 0.08	14.86 ± 0.06
(psia)	2166 ± 9	2156 ± 20	2150 ± 12	2155 ± 9
Vessel inlet temperature (K)	556.6 ± 4.0	557.8 ± 1.1	552.3 ± 0.8	552.4 ± 0.9
(°F)	542.5 ± 7.2	544.6 ± 2.0	534.7 ± 1.6	534.9 ± 1.6
Core ΔT (K)	33.1 ± 4.3	19.2 ± 2.1	26.8 ± 1.3	26.8 ± 1.2
(°F)	59.6 ± 7.7	34.6 ± 3.8	48.2 ± 2.3	48.2 ± 2.2
Reactor power (MW)	36.0 ± 1.2	50 ± 1	45.9 ± 1.2	46.0 ± 1.2
Maximum linear heat generation rate (kW/m)	40.1 ± 3.0	52.7 ± 3.7	46.0 ± 3.5	45.8 ± 3.5
(kW/ft)	12.2 ± 0.9	16.1 ± 1.1	14.0 ± 1.1	14.0 ± 1.1
Accumulator pressure (MPa)	4.28 ± 0.06	—	1.66 ± 0.05	4.50 ± 0.05
(psia)	621 ± 9	—	241 ± 7	653 ± 7

Table 3. Sequence of events for LOFT Experiments L2-5, L3-6/L8-1, L5-1, and L8-2

	Time After Initiation (s)			
Event	L2-5	L3-6/L8-1	L5-1	L8-2
Experiment initiated[a]	0	0	0	0
Reactor scrammed	0.24 ± 0.01	-5.8 ± 0.2	0.17 ± 0.01	0.10 ± 0.05
Primary coolant system starts to saturate	0.043 ± 0.01	28.5 ± 0.2	0.2 ± 0.1	0.2 ± 0.1
Primary coolant pump turned off	0.94 ± 0.01	2371.4 ± 0.2	4.0 ± 0.5	3.2 ± 0.5
Cladding temperature exceeds saturation temperature	190 ± 0.5[b]	2394.6 ± 0.2	108.4 ± 1.0	112.0 ± 0.5
Maximum cladding temperature reached	383 ± 2[b]	2465.8 ± 0.2	198.0 ± 2.0	299.1 ± 0.5
Core quench initiated	380 ± 1[b]	2466 ± 1	188.1 ± 0.5	299.5 ± 0.5
Core quench complete	430 ± 1[b]	2472.6 ± 0.2	214.0 ± 1.0	306.4 ± 0.5

a. Experiment initiation defined as the time when the break was opened.

b. For the second heatup.

time, the cladding temperature started to exceed the saturation temperature, as shown in Figure 5, indicating an approach to ICC. The mass depletion continued until the core was fully uncovered. The time from initiation of the core uncovery to its completion was 73 s, which allowed time for operator action to evaluate the state of the core and reinitiate ECCS injection. At ∿347 s, ECCS injection reversed the mass loss, and the bottom-up core quench started at ∿380 s. The core was completely quenched by 430 s. The maximum cladding temperature attained was ∿940 K (1230°F), at the nearly adiabatic heatup rate of 3 K/s (5.4°F/s). At this heatup rate, the 10 CFR 50 Appendix K limit of 1475 K (2200°F) (Reference 1) would have been reached within an additional 180 s (3 min) if the ECCS injection had not been reinitiated. Thus, this experiment fulfills the requirements of the working definition of ICC stated in the Introduction.

Because the TC TE-5UP-4 response was similar to that for the other core exit TCs, and showed the maximum response to core heatup, it was chosen as the representative core exit TC in this and the following discussions. The response of this TC to the ICC condition described above for experiment L2-5 is compared in Figure 6 with saturation temperatures calculated from upper-plenum pressures. As shown, the core exit TC temperature remained approximately at the saturation temperature until 370 s, when the core exit TC temperature increased to 490 K (423°F), at a rate of 2.3 K/s (4.2°F/s). The same core exit temperature is compared in Figure 7 with cladding temperatures measured at elevations of 1.57 m (62 in.) and 0.66 m (26 in.) above the bottom of the core. The former elevation corresponds to the top of the fuel; the latter, to the elevation of maximum core power and temperature. As shown in the figure, the maximum core exit fluid temperature approximated the cladding temperature at the top of the core. The core exit TC temperature, however, was 450 K (810°F) lower than the maximum cladding temperature measured during the transient. In addition, the core exit TC did not start to respond to the ICC condition until 380 s. This response was 180 s (3 min) after core uncovery began, as shown in Figure 7, and occurred after the reinitiated ECCS injection had started to quench the core, as shown in Figure 8. These results, along with similar results from the other three experiments analyzed, are summarized in Table 4. The reasons for the delay in core exit TC response are discussed below.

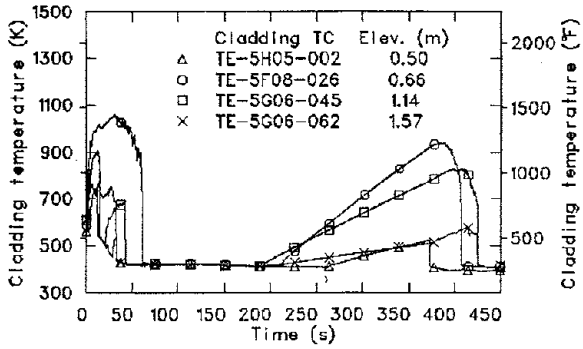

Figure 5. Typical cladding temperatures during the Experiment L2-5 blowdown and second heatup.

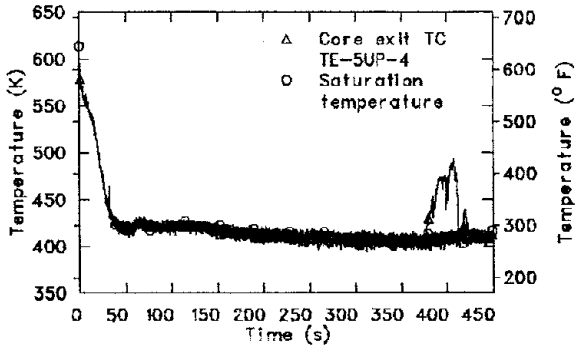

Figure 6. Typical core exit thermocouple response and saturation temperature during Experiment L2-5.

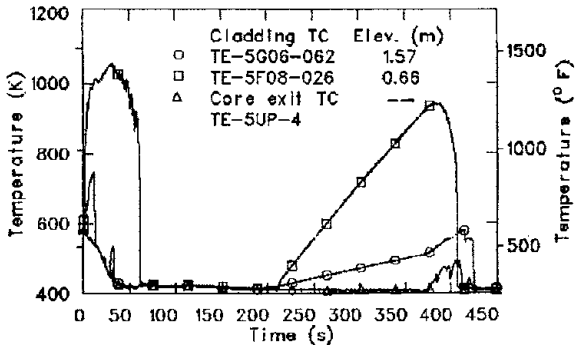

Figure 7. Cladding temperatures at elevations of 1.57 and 0.66 m and typical core exit thermocouple response during Experiment L2-5.

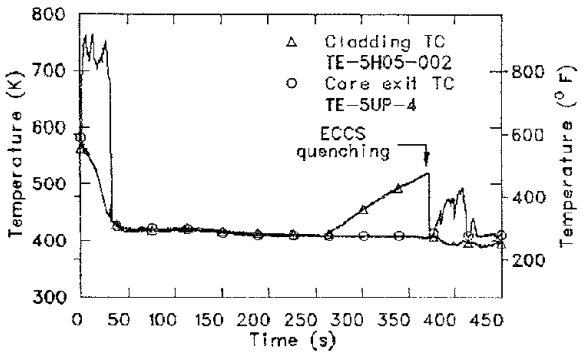

Figure 8. Cladding temperature at the 0.05-m elevation and typical core exit thermocouple response during Experiment L2-5.

At 144 s, when the high-pressure injection system flow was stopped, the collapsed liquid level was 1.19 m (46.9 in.) above the bottom of the core. At 190 s, when the core started to heat up, the collapsed liquid level was at 0.91 m (35.8 in.) above the core bottom, and the froth or mixture level was just at the core top [1.68 m (66.0 in.) above the core bottom]. During the time from 144 to 190 s, the two-phase mixture that existed in the upper-plenum region deposited films of water on surfaces in the upper plenum. Based on Oak Ridge National Laboratory (ORNL) test results[14] and INEL Semiscale experiments,[15] it appears that these water films gradually drained by gravity toward the core and continually coated the core exit TCs. The water film caused the core exit TCs to read the saturation temperature even though superheated vapor was being generated and was flowing past the TCs because of the continuing core uncovery. The ORNL results were obtained from testing of thermal devices that measure reactor vessel liquid level.

Table 4. Response of LOFT core exit thermocouple to core uncovery

Experiment	Δt[a] (s)	ΔT_{max}[b] (K) (°F)	$\Delta T_{1.57}$[c] (K) (°F)
L2-5	182 ± 1[d]	425 ± 8 765 ± 15	65 ± 8 117 ± 15
L3-6/L8-1	35 ± 1	125 ± 8 225 ± 15	15 ± 8 27 ± 15
L5-1	28 ± 1	135 ± 8 243 ± 15	95 ± 8 171 ± 15
L8-2	30 ± 1	340 ± 8 612 ± 15	90 ± 8 162 ± 15

a. Δt = time delay between initiation of core uncovery (measured by cladding temperature departure from saturation temperature) and core exit temperature response.

b. ΔT_{max} = difference between the maximum cladding temperature in the core and the maximum core exit thermocouple response.

c. $\Delta T_{1.57}$ = difference between the maximum cladding temperature measured at the 1.57-m (62-in.) elevation and the maximum core exit thermocouple response.

d. The core exit thermocouple did not respond to the core uncovery until after the core quench initiated.

The Semiscale results were obtained in a study of the efficacy of primary coolant system feed and bleed. In each case, a liquid film covering a temperature transducer reduced the ability of the transducer to measure vapor temperature.

During the time of the core uncovery before reinitiation of ECCS injection in Experiment L2-5, the vapor velocities were too low to strip the water film off the core exit TCs. [The fluid velocity was below the turbine velocity transducer deadband. A maximum velocity of 3 m/s (7 ft/s) was calculated from an energy balance.] Thus, decreasing core mixture level, increasing cladding temperatures, and static core exit TC response continued throughout the core uncovery phase. When the ECCS water started entering the hot, voided core, however, it was quickly vaporized. This vaporization resulted in a sudden increase in upper-plenum steam velocity [up to 7 m/s (23 ft/s)] measured by the turbine meter (Figure 9) and corroborated by the drag disc measurements (Figure 10), which are also sensitive to velocity. This rapidly moving steam displaced the nearly stagnant superheated vapor in the core and moved it into the upper plenum. As it exited the core, this superheated steam transferred part of its superheat to the upper core cladding. This reverse heat transfer is indicated in Figure 11 as a sudden acceleration, at about 375 s, of the rate of increase of cladding temperature beyond the rate calculated for adiabatic rod heatup alone, at the 1.47-m (58-in.) elevation. This superheated steam also stripped the liquid film off the core exit TCs, enabling the TCs to start measuring the vapor temperatures as shown in Figure 8.

In summary, the core exit TCs did not respond to ICC conditions in the core until the water film was stripped off. The potential for drying the core exit TCs was provided by superheated vapor driven out of the upper parts of the core by ECCS water flashing to steam in the bottom of the core. Had the ECCS injection not been initiated, it is conceivable that the cladding in the hottest region of the core could have heated up to unacceptable levels with no indication of the ICC condition by the core exit TC measurements.

Experiment L3-6/L8-1

Experiment L3-6/L8-1 was a small-break experiment in which the primary coolant pumps were left on during essentially all of the blowdown phase.[10,11]

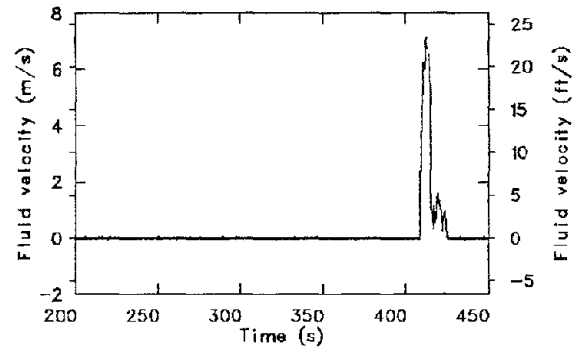

Figure 9. Upper-plenum fluid velocity during the Experiment L2-5 second heatup.

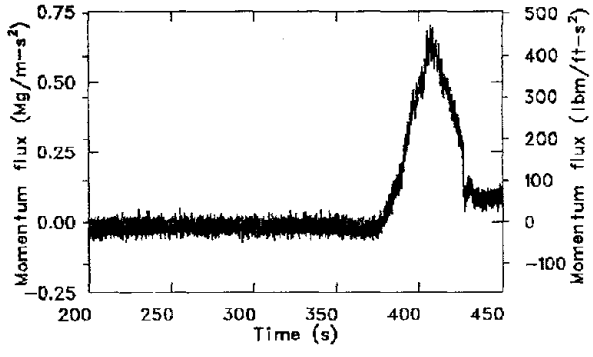

Figure 10. Upper-plenum fluid momentum flux during the Experiment L2-5 second heatup.

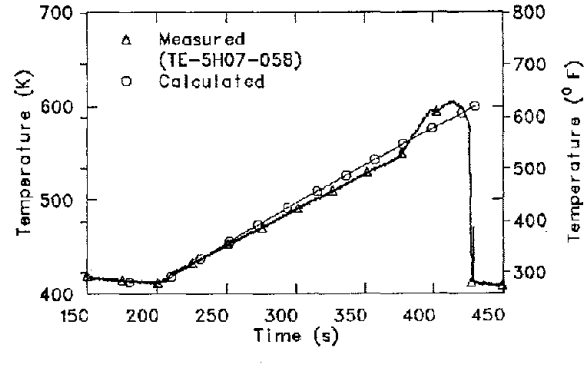

Figure 11. Measured cladding temperature and calculated adiabatic heatup temperature at the 1.47-m elevation during Experiment L2-5.

(This experiment was conducted in conjunction with a pumps-off experiment[16,17] to measure the effect of pump operation on primary coolant system response, especially mass inventory, during a small-break LOCA.) As long as the pumps were running, the core was adequately cooled by forced convection of a two-phase mixture that was characterized by a steadily increasing void fraction. It is expected that continued voiding would have eventually resulted in inadequate cooling even with forced convection. Prior to this occurrence, however, the pumps were turned off [2370 s (39 min)], at which time the reactor vessel void fraction exceeded 95%. In the subsequent absence of forced convection, the two-phase mixture rapidly stratified, uncovering the entire core within 1 min, as evidenced by the cladding heatup shown in Figure 12.

The core uncovery was allowed to persist ∿1 min before ECCS injection was initiated. ECCS injection quenched the core within an additional 11 s. As shown in Figure 13, the core exit TC response

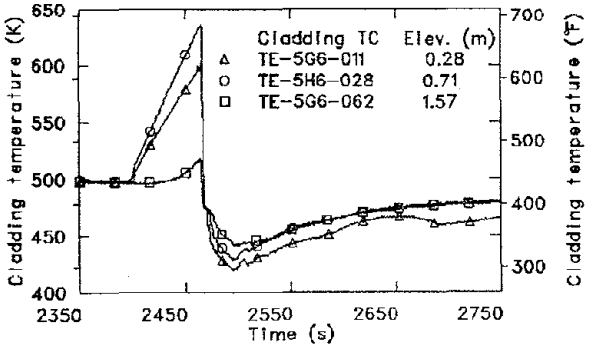

Figure 12. Typical cladding temperatures during Experiment L3-6/L8-1.

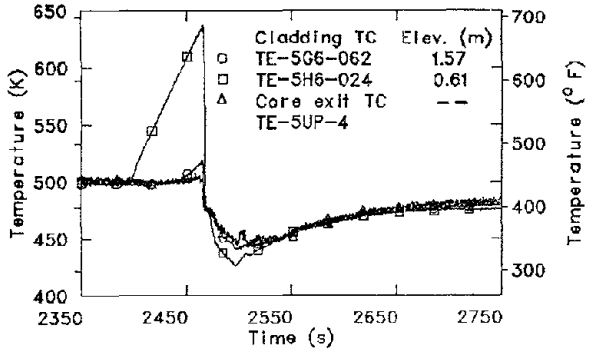

Figure 13. Cladding temperatures at elevations of 1.57 and 0.61 m and typical core exit thermocouple response during Experiment L3-6/L8-1.

to the core uncovery was delayed ∿35 s and the maximum temperature recorded by these TCs was 125 K (225°F) less than that reached in the hottest portion of the core [0.61-m (24-in.) elevation]. The temperature difference with respect to a cladding TC in the upper core [1.57-m (62-in.) elevation], however, was 15 K (27°F)—again demonstrating that the core exit TCs respond to either saturation conditions or core exit cladding temperatures rather than to temperatures in the hottest core region. These results are summarized in Table 4.

Experiments L5-1 and L8-2

Experiments L5-1 and L8-2 were intermediate-break LOCA simulations that were initiated from representative PWR conditions and that simulated the rupture of a 14-in. Schedule-160 ECCS pipe.[12,13] The break was noncommunicative in that only the broken-loop cold-leg quick-opening blowdown valve was opened. The primary coolant pumps were stopped coincident with reactor scram in both experiments and remained off throughout Experiment L5-1. The differences between these two experiments were in the ECCS operation and primary coolant pump operation as summarized in Table 1. As shown by the cladding TC response in Figure 14, the Experiment L5-1 core uncovery initiated at 108 s (1.8 min) and continued until 214 s (3.6 min), when the core was quenched. In the interim, the core was 95% uncovered at 186 s (3.1 min). The core exit TC response to the core uncovery is shown in Figure 15, along with the cladding temperatures measured at elevations of 1.57-m (62-in., upper core) and 0.99-m (39-in., maximum-temperature region). The delay time between core uncovery and core exit TC response was 28 s. The differences between the maximum core exit TC

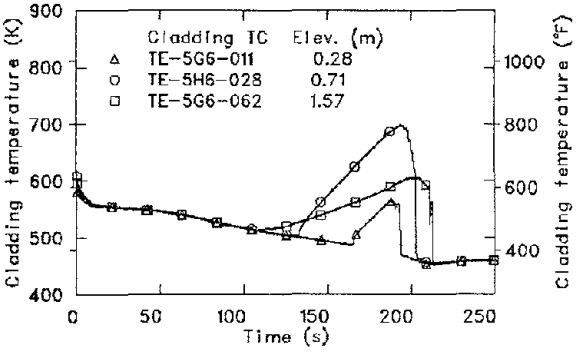

Figure 14. Typical cladding temperatures during Experiment L5-1.

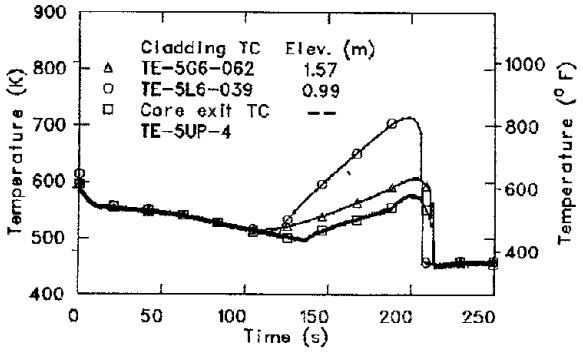

Figure 15. Cladding temperatures at elevations of 1.57 and 0.99 m and typical core exit thermocouple response during Experiment L5-1.

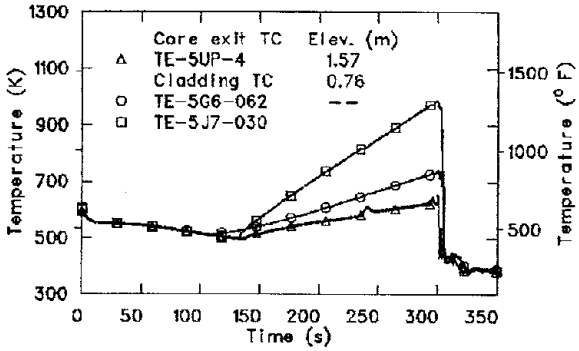

Figure 17. Cladding temperatures at elevations of 1.57 and 0.76 m and typical core exit thermocouple response during Experiment L8-2.

response and the maximum cladding temperatures at the 1.57-m (62-in.) and 0.99-m (39-in.) elevations were 95 K (171°F) and 135 K (243°F), respectively.

In Experiment L8-2, ECCS injection was delayed to allow a more detailed examination of the core thermal response to the uncovery and to measure the cooling effects of restarting the primary coolant pump with a voided, hot core. In this case, the uncovery lasted from 112 s (1.9 min) to 306 s (5.1 min)—a net uncovery time of 194 s (3.2 min)—and the entire core was allowed to uncover. Consequently, as shown in Figures 16 and 14, the maximum cladding temperature was much higher in Experiment L8-2 [987 K (1317°F)] than in Experiment L5-1 [715 K (828°F)]. Figure 17 compares the Experiment L8-2 core exit TC response with the cladding temperatures at the 1.57-m (62-in., upper core) and 0.76-m (30-in.) elevations, the latter corresponding to the maximum cladding temperature measured during this experiment. As in the other experiments, the core exit TC response was delayed (by 30 s) and reduced in magnitude with respect to cladding temperature. The core exit TC response was 340 K (612°F) less than the cladding TC response at the 0.76-m (30-in.) elevation and 90 K (162°F) less than the cladding TC response at the 1.57-m (62-in.) elevation.

Comparison of Results

In Experiments L3-6/L8-1, L5-1, and L8-2, the mechanism for removal of the liquid film from the TCs apparently involved the continuing primary coolant system depressurization, which caused the film to vaporize to steam. In these experiments, as shown in Figures 18, 19, and 20, the primary-system pressure continued to decrease in response to the break flow during the core uncovery, indicated in the figures by the increase in cladding temperature at the 0.61-m (24-in.) elevation. As shown in Figure 21, depressurization did not occur during the second heatup in Experiment L2-5, since the core

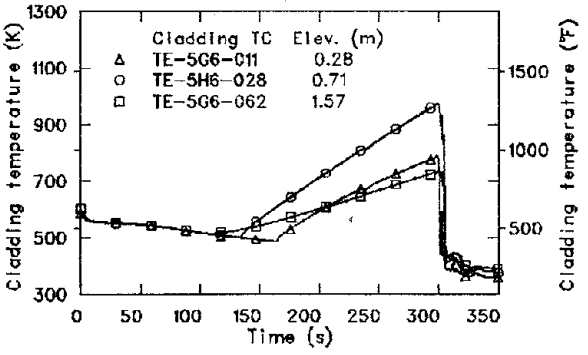

Figure 16. Typical cladding temperatures during Experiment L8-2.

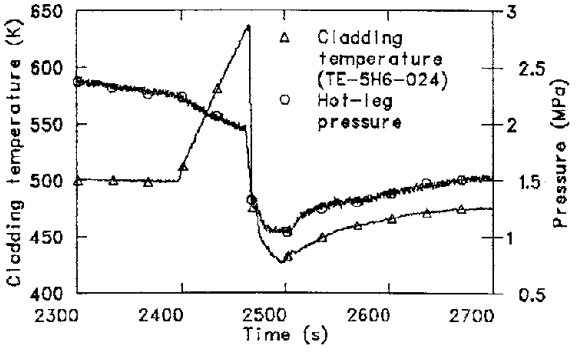

Figure 18. Experiment L3-6/L8-1 hot-leg pressure and maximum cladding temperature during core uncovery.

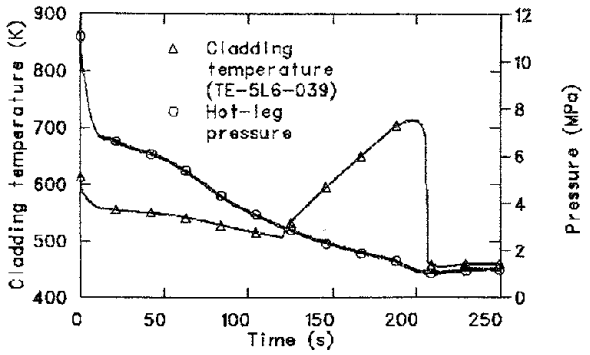

Figure 19. Experiment L5-1 hot-leg pressure and maximum cladding temperature during core uncovery.

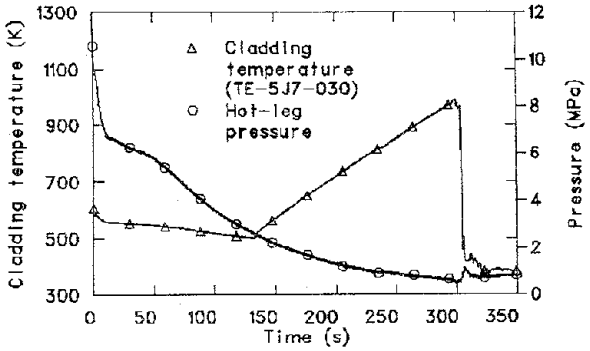

Figure 20. Experiment L8-2 hot-leg pressure and maximum cladding temperature during core uncovery.

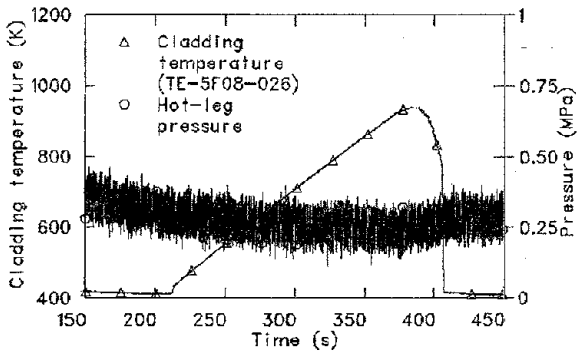

Figure 21. Experiment L2-5 hot-leg pressure and maximum cladding temperature during second heatup.

uncovery did not initiate until the primary-system pressure had equilibrated with that in the blowdown suppression tank. Thus, the delay in the response of the core exit TCs in Experiments L3-6/L8-1, L5-1, and L8-2 was much less than that in Experiment L2-5.

In summary, although the core exit TC responses to the core uncoveries in Experiments L3-6/L8-1, L5-1, and L8-2 were fairly close to the measured cladding temperatures at the 1.57-m (62-in.) elevation, the core exit TC responses from all four experiments were in general delayed with respect to initiation of the uncovery and reduced in magnitude relative to the maximum cladding temperatures attained in the core. The water film that tended to inhibit the response of these TCs to superheated vapor exiting the core had to be removed before the TCs could respond to the superheat. Also, the temperatures that the core exit TCs did respond to (after the film was removed) corresponded to cladding temperatures in the upper core region, which were much less than those in the hottest core regions.

CONCLUSIONS

Core exit TC response has been reviewed for four LOFT core uncoveries. It is concluded that care should be taken in the use of core exit TC measurements to detect ICC or the approach to ICC.

In the core uncoveries studied, slow drainage of liquid from the upper plenum coated the core exit TCs with a liquid film after the froth level had subsided. For a core exit TC to respond to the ICC condition, this film had to be removed by additional heat flux to boil it off, by primary system depressurization to flash the film to vapor, or by sufficient steam velocity to strip it off. When the film was removed, the core exit TCs measured the vapor temperatures at the core exit. However, these core exit vapor temperatures tended to follow the cladding temperatures in the upper regions of the core. In the LOFT PWR, the upper core regions are in a low decay power generation location and the decay power generation at the hottest part of the core is much higher. The vapor temperatures at the core exit can thus be several hundred Kelvin lower than those in the hotter core regions.

Certainly, if an ICC condition is indicated by core exit TCs, the operator would be prudent to conclude that core damage is imminent. However, because of the quenching effect studied here, and without a reliable correlation of core exit TC response with temperatures in the hottest core regions, the use of the core exit TC response alone would be insufficient, without sufficient corroborating information, to conclude the absence of ICC. Any use of the core exit TCs for this purpose must be predicated on conservative temperature limits that take into account core—core-exit temperature differentials and the quenching effect of water films on the thermocouples.

In summary, two general limitations have been identified regarding the ability of core exit fluid TCs to monitor a core uncovery. First, there was a delay between the core uncovery and the TC response. This delay ranged from 28 to 182 s in the four LOFT LOCA simulations, and could have been even longer in one case, had the reactor operators not initiated core reflood. The delay is judged to be caused by a film of water that coats the TC and must be removed before the TC can respond to the vapor superheat. The film of water exists due to slow drainage of liquid from the upper plenum. Although the magnitude of these delays is acceptable under the controlled conditions in the LOFT system, these delay times may differ in commercial systems and should be accounted for in the use of core exit TC response to predict or measure ICC. Since it is expected that ICC will initiate in the hottest core regions, any delay or inadequacy in measuring the temperature of these regions must be considered when analyzing potential methods for ICC detection.

Second, the measured core exit TC response was several hundred Kelvin lower than the maximum cladding temperatures in the core. This temperature difference results from the vapor superheat at the core exit being limited by the cladding temperatures near the core exit. In the LOFT system, these cladding temperatures were up to 360 K (648°F) lower than those in the high-power regions near the core center.

In conclusion, any procedure that relies on the response of core exit fluid TCs to monitor a core uncovery should take these two limitations into account. There may be accident scenarios in which these TCs would not detect inadequate core cooling that preceded core damage.

REFERENCES

1. U.S. Atomic Energy Commission, "Licensing of Production and Utilization Facilities," Appendix K, "ECCS Evaluation Models," *Code of Federal Regulations, Title 10 Atomic Energy, Part 50*, Docket No. RM-50-1, January 1, 1976.

2. *TMI-2 Lessons Learned Task Force Status Report and Short-Term Recommendations*, NUREG-0578, July 1979.

3. *U.S. NRC Regulatory Guide 1.97*, Rev. 1, December 1980.

4. Minutes of a meeting of the U.S. Nuclear Regulatory Commission, "Discussion of Reactor Vessel Water Level Indicators," January 8, 1982.

5. *Inadequate Core Cooling Instrumentation Using Differential Pressure for Reactor Vessel Level Measurements*, NUREG/CR-2628, March 1982.

6. D. L. Reeder, *LOFT System and Test Description (5.5 ft Nuclear Core LOCEs)*, NUREG/CR-0247, TREE-1208, July 1978.

7. L. J. Ybarrondo, et al., "Examination of LOFT Scaling," 74-WA-HT-53, *Proceedings of the Winter Meeting of the American Society of Mechanical Engineers, New York, November 17-22, 1974*, CONF-741104.

8. J. P. Adams, *Quick-Look Report on LOFT Nuclear Experiment L2-5*, EGG-LOFT-5921, June 1, 1982.

9. P. D. Bayless and J. M. Divine, *Experiment Data Report for LOFT Large Break Loss-of-Coolant Experiment L2-5*, NUREG/CR-2826, EGG-2210, August 1982.

10. G. E. McCreery, *Quick-Look Report on LOFT Nuclear Experiment L3-6/L8-1*, EGG-LOFT-5318, Rev. 1, July 1981.

11. P. D. Bayless and J. M. Carpenter, *Experiment Data Report for LOFT Nuclear Small Break Experiment L3-6 and Severe Core Transient Experiment L8-1*, NUREG/CR-1868, EGG-2075, January 1981.

12. J. P. Adams, *Quick-Look Report on LOFT Nuclear Experiments L5-1 and L8-2*, EGG-LOFT-5625, October 1981.

13. D. B. Jarrell and J. M. Divine, *Experiment Data Report for LOFT Intermediate Break Experiment L5-1 and Severe Core Transient Experiment L8-2*, NUREG/CR-2398, EGG-2136, November 1981.

14. J. E. Hardy, et al., *Evaluation of Thermal Devices for Detecting In-Vessel Coolant Levels in PWRs*, NUREG/CR-2673, ORNL/TM-8306, August 1982.

15. D. J. Shimeck et al., *Analysis of Primary Feed and Bleed Cooling in PWR Systems*, EGG-SEMI-6022, September 1980.

16. J. P. Adams, *Quick-Look Report on LOFT Nuclear Experiment L3-5/L3-5A*, EGG-LOFT-5242, October 1980.

17. L. T. L. Dao and J. M. Carpenter, *Experiment Data Report for LOFT Nuclear Small Break Experiment L3-5/L3-5A*, NUREG/CR-1695, EGG-2060, November 1980.

APPENDIX

REACTOR VESSEL THERMAL-HYDRAULIC CONDITIONS DURING THE SECOND HEATUP OF LOFT EXPERIMENT L2-5

APPENDIX

REACTOR VESSEL THERMAL-HYDRAULIC CONDITIONS DURING THE SECOND HEATUP OF LOFT EXPERIMENT L2-5

This appendix describes calculations of the thermal-hydraulic aspects of the core heatup that occurred during the LOFT Experiment L2-5 second core uncovery. The experiment conduct is described in detail in the main body of this report and in References A-1 and A-2. Only the calculations needed to determine the phenomena of core heatup and core exit thermocouple (TC) response are included here. The calculations indicate that the core underwent a dryout type boiling transition—which proceeded from the core top to the core bottom. During the dryout, the core exit TCs were wetted by a liquid film until significant flow of superheated steam evaporated and swept off the film on several TCs about 180 s after fuel rod dryout first occurred. The core exit TCs then showed a temperature rise. The core was then quenched by operator initiated coolant flow from the high-pressure and low-pressure injection systems.

Calculation Methodology

The significant thermal-hydraulic calculations necessary to quantify and determine the mechanisms of core heatup and core exit TC response are: core heat transfer; liquid mass and void fraction in the reactor vessel, core, and downcomer; liquid entrainment and deposition; upper-plenum countercurrent flow limiting conditions; and fuel rod top quenching. The required calculations and the sequence in which they were performed are

1. Critical heat flux (CHF); to show that the transition is due to dryout rather than to CHF.

2. Reactor vessel mass; from a mass balance obtained by integrating measured mass flow rates into and out of the reactor vessel and summing.

3. Collapsed liquid level and void fraction in the core and downcomer at 190 s; from reactor vessel mass.

4. Core and downcomer steam velocities.

5. Core liquid froth level as a function of collapsed liquid level and steam velocity, using drift flux and the data of Shires et al.[A-3] and Annunziato et al.[A-4]

6. Collapsed liquid level at which the froth level just uncovers the core; to compare with the level calculated in Step 3.

7. Downcomer froth level; using drift flux.

8. Reactor vessel wall heat transfer summed with core decay power; to determine mass of water evaporated in core and relate to the core void fractions calculated above.

9. Droplet entrainment rate and flux above the froth level; using core exit steam velocity.

10. Deposition rate of droplets on core exit TCs and minimum steam superheating necessary to evaporate deposited droplets.

11. Upper-plenum countercurrent flow limiting (CCFL) conditions, using the data of Jacoby and Mohr[A-5] and Sun,[A-6] to compare with indications of CCFL conditions in the experiment data.

12. Fuel rod top quench velocity; to compare with data for upper core elevations and relate to upper-plenum liquid inventory.

The major assumptions employed in the calculations are

1. Flow is quasi-steady state.

2. Pressure is approximately constant between 100 and 400 s (the data indicate this).

3. The liquid and vapor densities, ϱ_f and ϱ_g, are constant and at saturation values.

4. The downcomer collapsed liquid level is equal to the core collapsed liquid level

(static equilibrium assumption). RELAP5 calculations[A-7] and hand calculations of pressure losses and pressure differentials support this assumption.

5. Three-dimensional aspects, such as flow distribution in the outer bundles compared with the center bundle, are not considered. Only core average flow and flow in the center bundle are analyzed.

Critical Heat Flux. To determine if the boiling transition during core uncovery (190 to 425 s) was due to CHF in pool boiling or to dryout, we determined (a) if the maximum mass flux out of the core is within the range expected for pool boiling and (b) if the maximum heat flux exceeds that required for CHF in pool boiling.

The maximum mass flux, $\dot{M}/A_{x_{rod}}$, where $\dot{M}$ is the maximum mass flow rate out of the core per fuel rod, and $A_{x_{rod}}$ is the cross-sectional flow area per fuel rod, is given by

$$\frac{\dot{M}}{A_{x_{rod}}} = \left(\frac{q}{A}\right)_{rod\ max} \frac{A_{rod}}{h_{fg}} \left(\frac{1}{A_{x_{rod}}}\right) \qquad (1)$$

where A_{rod} is the surface area of a fuel rod, h_{fg} is the specific heat of vaporization, and $(q/A)_{rod\ max}$ is the maximum heat flux per fuel rod. The maximum heat flux is calculated from the decay heat as follows:

$$\left(\frac{q}{A}\right)_{rod\ max} = \frac{\text{decay heat}}{\pi d_{rod}}$$

where d_{rod} is the rod diameter.

The decay heat at 200 s is assumed to be typical of that during the core uncovery phase and is ~2.5% of the initial maximum linear heat generation rate of 40 kW/m (12 kW/ft). Given a fuel rod diameter of 0.01072 m (0.0352 ft), the maximum heat flux is then 29.7 kW/m^2 (2.76 kW/ft^2). Substituting in Equation (1), and using A_{rod} = 0.0565 m^2 (0.608 ft^2), h_{fg} = 2140 kJ/kg (919 Btu/lbm), and A_{xrod} = 1.142 x 10^{-4} m^2 (1.23 x 10^{-3} ft^2), the maximum mass flux is then 6.87 kg/m^2·s (1.408 lbm/ft^2·s). For a mass flux this small, pool boiling is the appropriate heat transfer mechanism.

The CHF for pool boiling is then calculated from the Zuber CHF correlation (Reference A-8):

$$\left(\frac{q}{A}\right)_{CHF(Zuber)} = 0.18\varrho_g h_{fg}\left(\frac{\sigma(\varrho_f - \varrho_g)g}{\varrho_g^2}\right)^{0.25} \left(\frac{\varrho_f}{\varrho_f + \varrho_g}\right)^{0.5}$$

where σ is the surface tension and g is the gravitational constant. The calculated CHF is 2.57 x 10^6 W/m^2 (2.39 x 10^5 W/ft^2). At 200 s, however, the maximum heat flux calculated from the core decay heat was 2.97 x 10^4 W/m^2 (2.76 x 10^3 W/ft^2), which is less than the calculated Zuber CHF for pool boiling. Thus, the mechanism for the core heatup is a dryout rather than a pool boiling type of CHF.

Reactor Vessel Mass Inventory. The reactor vessel mass inventory (M_{RV}) was calculated as a function of time (t) as follows:

$$M_{RV}(t) = M_o + \int_o^t \dot{M}_{ILCL}dt - \int_o^t \dot{M}_{ILHL}dt - \int_o^t \dot{M}_{BLHL}dt - \int_o^t \dot{M}_{BLCL}dt + \int_o^t \dot{M}_{ECCS}$$

where

M_o = initial reactor vessel mass (kg)

$\dot{M}$ = mass flow rate (kg/s)

ILCL = intact-loop cold leg

ILHL = intact-loop hot leg

BLCL = broken-loop cold leg

BLHL = broken-loop hot leg

ECCS = Emergency Core Cooling System.

The resultant reactor vessel mass inventory over time is shown in Figure A-1. However, the mass flow rates measured after 30 s were in general lower than the measurement uncertainty. After 30 s therefore, the mass inventories in Figure A-1 must be considered to be qualitative only. To obtain quantitative mass inventories for times of interest in this report, the following is noted: at 450 s, the reactor vessel was full to the nozzles, limiting the mass inventory to 2230 kg (4920 lbm). The mass inventory shown in Figure A-1, however, shows 2700 kg (5950 lbm) at this time, or ∿470 kg (∿1040 lbm) more than would fill the vessel. Therefore, approximate reactor vessel inventories for times after 30 s can be obtained by subtracting 470 kg (1040 lbm) from the values in Figure A-1.

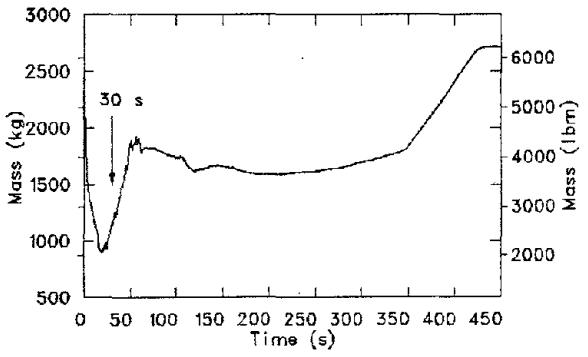

Figure A-1. Calculated reactor vessel mass inventory during Experiment L2-5.

Collapsed Liquid Level. Using the reactor vessel mass inventories corrected as above, the collapsed liquid levels prior to and during the heatup can be calculated. For this calculation, it is assumed that (a) downcomer and reactor vessel collapsed liquid levels are equal (static equilibrium) and (b) no mass is stored in the upper plenum or elsewhere in the reactor vessel, independent of that associated with core liquid frothing.

Collapsed Liquid Level Prior to Heatup (144 s, High-Pressure Injection Turned Off). At 144 s, the corrected reactor vessel mass was 1200 kg (2650 lbm). The liquid volume corresponding to this mass is 1.274 m^3 (45.0 ft^3) and the corresponding reactor vessel collapsed liquid level is 1.19 m (47 in.) above core bottom.

Collapsed Liquid Level During Heatup (190 s, Heatup Begins). At 190 s, the corrected reactor vessel mass was 1120 kg (2470 lbm), which corresponds to an average core void fraction of 0.46. The liquid volume corresponding to this reactor vessel mass is 1.19 m^3 (42.0 ft^3) and the corresponding reactor vessel liquid level is 0.914 m (36 in.) above core bottom. The collapsed liquid level therefore decreased at an average of 0.0061 m/s (0.24 in./s) between 144 and 190 s. This rate is used below in the reactor vessel energy balance calculation.

Core and Downcomer Steam Velocities

Steam Velocities at 190 s. The rate of formation of steam and the resulting steam velocity is determined by the rate of heat transfer to the liquid. The steam velocity is calculated to determine if it is sufficient to hold up liquid in the upper plenum. It is assumed that froth covers the core and that core decay power, P_{core}, at 190 s is 0.9 MW. The reactor vessel heat transfer from hot structural materials to liquid below the upper-plenum level, P_{RV}, is calculated by RELAP5 to be 1.45 MW. The RELAP5 reactor vessel wall heat fluxes correspond closely to conduction limited solutions for the components. The major heat source in the downcomer is assumed to be the reactor vessel filler block. P_{RV} is distributed between the core, $P_{RV\ into\ core}$, and the downcomer, $P_{RV\ into\ DC}$, approximately as follows, where the downcomer is taken to include the filler gap and the core bypass:

$$P_{RV\ into\ core} = 0.15\ MW$$

$$P_{RV\ into\ DC} = 1.3\ MW\ .$$

Using these values, outlet steam velocities, $V_{g_{out}}$, for the core and downcomer are calculated as follows:

$$V_{g_{out\ core}} = \frac{P_{core} + P_{RV\ into\ core}}{A_{x_{core}} \varrho_g h_{fg}}$$

and

$$V_{g_{out\ DC}} = \frac{P_{RV\ into\ DC}}{A_{x_{DC}} \varrho_g h_{fg}}$$

where $A_{x_{core}}$ and $A_{x_{DC}}$, the cross-sectional flow areas for the core and downcomer, are 0.165 and 0.171 m^2 (1.78 and 1.84 ft^2), respectively.

Substituting, we get

$$V_{g_{\text{out core}}} = 2.14 \text{ m/s} = 7.02 \text{ ft/s}$$

and

$$V_{g_{\text{out DC}}} = 2.04 \text{ m/s} = 6.69 \text{ ft/s} .$$

The average core steam velocity, $\bar{V}_{g_{core}}$, is calculated by assuming that the $P_{RV \text{ into core}}$ component is from the lower plenum and the steam generated from this component enters the core inlet. Then

$$\bar{V}_{g_{core}} = V_{g_{\text{out core}}} \left[\frac{1}{2} \left(\frac{P_{\text{core}}}{P_{\text{core}} + P_{\text{RV into core}}} \right) + \frac{P_{\text{RV into core}}}{P_{\text{core}} + P_{\text{RV into core}}} \right]$$

$$= 2.14 \frac{\text{m}}{\text{s}} \left[\frac{1}{2} \left(\frac{0.9 \text{ MW}}{1.05 \text{ MW}} \right) + \left(\frac{0.15 \text{ MW}}{1.05 \text{ MW}} \right) \right]$$

$$= 1.22 \text{ m/s} = 4.00 \text{ ft/s} .$$

The average steam velocity in the downcomer, $\bar{V}_{g_{DC}}$, is calculated by assuming that the heat transfer to liquid below the downcomer inlet, $P_{RV \text{ below DC}}$, is 0.2 MW. This contribution is assumed to be from the lower plenum and from the bottom of the reactor vessel filler. Then

$$\bar{V}_{g_{DC}} = V_{g_{\text{out DC}}} \left[\frac{1}{2} \left(\frac{P_{\text{RV into DC}}}{P_{\text{RV into DC}} + P_{\text{RV below DC}}} \right) + \frac{P_{\text{RV below DC}}}{P_{\text{RV into DC}} + P_{\text{RV below DC}}} \right]$$

$$= 2.04 \frac{\text{m}}{\text{s}} \left[\frac{1}{2} \left(\frac{1.1 \text{ MW}}{1.3 \text{ MW}} \right) + \frac{0.2 \text{ MW}}{1.3 \text{ MW}} \right]$$

$$= 1.18 \text{ m/s} = 3.86 \text{ ft/s} .$$

Core Exit Steam Velocity After 190 s. The core exit steam velocity after 190 s is calculated by assuming that only steam is present above the froth level (this is consistent with the calculated rate of droplet entrainment above the froth level). Heat transfer from the fuel rods below the froth level boils the fluid and heat transfer above the froth level superheats the steam. Core exit steam velocity is then given by

$$V_{g_{\text{out core}}} = \left(\frac{P_{\text{core}_{\text{into froth}}}}{A_{x_{\text{core}}} \varrho_g h_{fg}} + V_{g_{\text{into core}}} \right) \frac{T_{g_{\text{out core}}}}{T_{\text{sat}}}$$

where

$P_{\text{core}_{\text{into froth}}}$ = decay power below froth level

$A_{x_{\text{core}}}$ = core cross-sectional area

$T_{g_{\text{out core}}}$ = vapor temperature at the core exit

T_{sat} = saturation temperature.

The results of this calculation are shown in Figure A-2, for a core exit steam temperature estimated to be equal to the average fuel rod temperature at the 1.24-m (49-in.) elevation. The significant feature of this calculation is that core

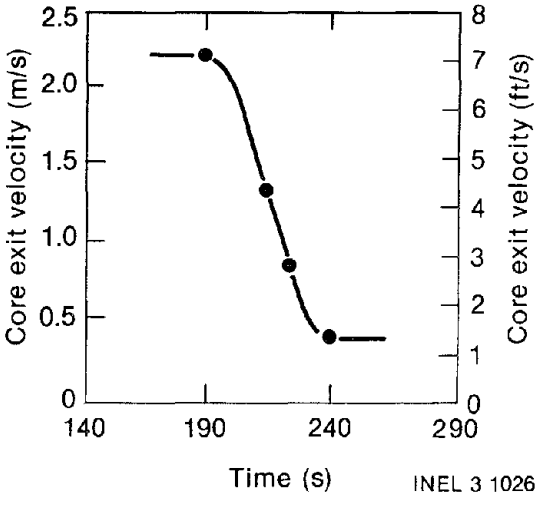

Figure A-2. Calculated core exit steam velocity during Experiment L2-5.

exit steam velocity decreases with time, and therefore the propensity for liquid entrainment and upper-plenum flooding also decreases with time after 190 s.

Core Froth Level. Before the core dries out starting at 190 s, the core is immersed in a boiling steam—water froth. The experimental study of Shires et al.[A-3] correlates the froth level, Y_S, of an electrically heated fuel rod bundle with average steam velocity ($\bar{V}_S$). Correlations of the average steam velocity with average void fraction for a 50% filled (collapsed liquid level) core are shown in Figure A-3. It is assumed that the core inlet fluid is at saturated conditions. This is supported by data that show the lower-plenum fluid is at the saturation temperature.

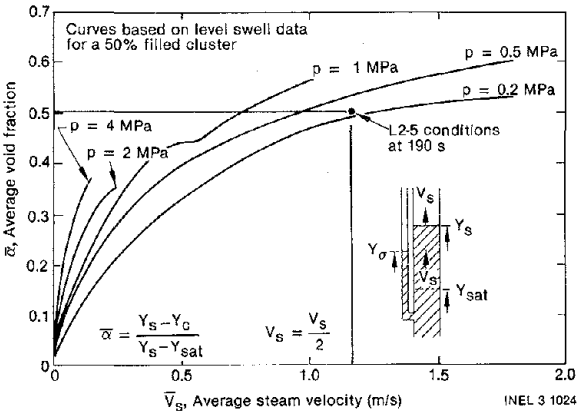

Figure A-3. Variation of average void fraction with average steam velocity—data of Shires, et al.[A-2]

For a froth level ≤ 1.68 m (≤ 5.5 ft) and $\bar{V} = 1.2$ m/s (3.9 ft/s)(see the steam velocity calculation), the average void fraction, $\bar{\alpha}$, is 0.5, from Figure A-3. According to the Shires equation, shown in Figure A-3, the froth level, Y_S, as a function of the collapsed liquid level, Y_C, is then

$$Y_S = 2.0Y_C = 1.68 \text{ m} = 5.5 \text{ ft} .$$

For L2-5 conditions, for $Y_S > 1.68$ m, Y_S is given by

$$Y_C/(1 - \bar{\alpha})$$

where

$$\bar{\alpha} \cong 1/(C_o + V_{gj}/\bar{V}_g)$$

C_o = distribution parameter = 1.20 (from Figure 8 in Reference A-3)

V_{gj} = drift flux = 0.83 m/s = 2.7 ft/s (chosen to agree with Reference A-3 data)

$\bar{V}_g$ = average steam velocity

$$= \frac{\bar{V}_{g_{core}} L_c + V_{g_{out\ core}} (Y_s - L_c)}{Y_s}$$

L_C = core length.

The calculated froth level as a function of collapsed liquid level for Experiment L2-5 is shown in Figure A-4.

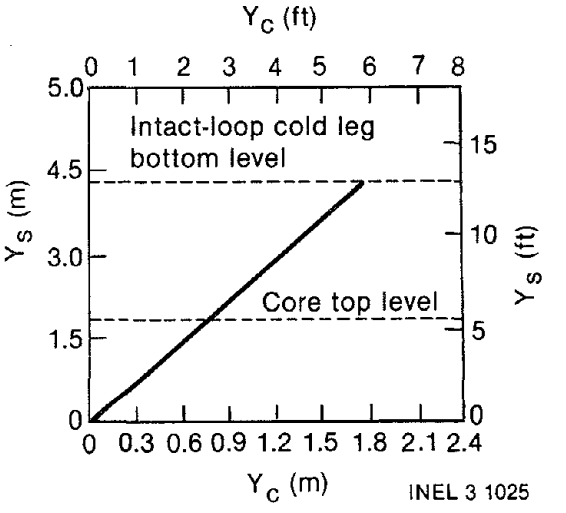

Figure A-4. Froth level, Y_S, versus collapsed liquid level, Y_C, for Experiment L2-5 conditions, using the data of Shires, et al.[A-2]

The average core void fraction can also be calculated by the method of Sun et al.[A-9] using a drift flux given by

$$V_{gj} = 2.9 \left[\frac{(\varrho_f - \varrho_g)\, \alpha\, g\, g_c}{\varrho_f^2} \right]^{0.25}$$

$$\cong 0.457 \text{ m/s} = 1.5 \text{ ft/s}$$

and $C_0 = 1.2$, as recommended by Lahey[A-8] for fully developed bubbly flow. Using this method, which integrates void fraction up each flow channel in the core, the average void fraction in the core is 0.53 for $Y_S = 1.68$ m (5.5 ft).

A third method of calculating the average void fraction in the core is recommended by Annunziato et al.,[A-4] based on experiments on uncovered core heat transfer using an electrically heated fuel rod bundle. This method uses the drift flux given by Lahey for bubbly flow, but uses $C_0 = 1.55$. For $Y_S = 1.68$ m (5.5 ft), this results in $\bar{\alpha} \cong 0.51$, which is close to the Shires value.

For Experiment L2-5, the average core void fraction obtained from experimental data at the beginning of core uncovery (190 s) was ~0.5. The three calculated values for void fraction are consistent with the experimental data. Therefore, the average core void praction is taken to be ~0.5 .

Downcomer Froth Level. During the core heatup period, there was no ECC injection and the downcomer collapsed liquid level was equal to the core collapsed liquid level plus or minus a small height that corresponded to the fluid flow head loss through the primary loop. (The sign depends on the direction of flow and is plus for loop positive flow and minus for loop negative flow). The difference in collapsed liquid levels is calculated by hand and by RELAP5 to be <2.5 cm (<1 in.). That the downcomer collapsed liquid level corresponds to the core liquid elevation is confirmed by the difference in measured pressure between the top and bottom of the downcomer, shown in Figure A-5. Although the pressure measurements are inaccurate due to transducer uncertainties, the difference is qualitatively believable.

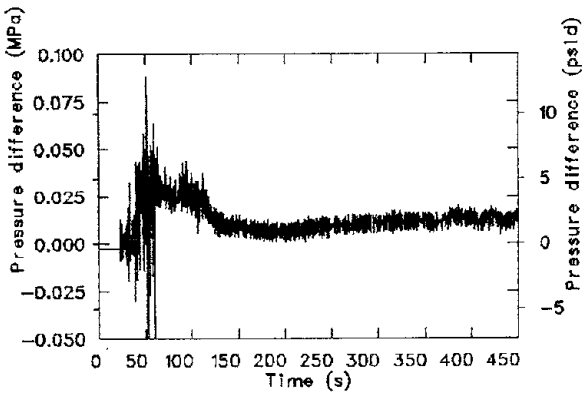

Figure A-5. Pressure difference between top and bottom of downcomer during Experiment L2-5.

The froth level in the downcomer is calculated from the drift flux for fully developed bubbly flow. At 190 s, for the collapsed liquid level at the mid-core elevation and the downcomer entrance 1.07 m (42 in.) below the core, as in the LOFT system, the calculated average void fraction in the downcomer is $\bar{\alpha}_{DC} \cong 0.64$. The corresponding froth level, Y_S, is ~5.30 m (17.4 ft), which is above the cold-leg nozzles [4.67 m (15.3 ft) above the downcomer entrance]. Therefore, core dryout was enhanced by mass flow out the reactor vessel through the intact-loop cold leg and broken-loop cold leg, as well as by evaporation. A more precise calculation of froth level can be made by integrating void fraction up the channel as described by Sun et al.[A-9] However, the froth level obtained in this calculation ($Y_S = 7.05$ m = 21.5 ft) is even higher. As shown in the next section, core decay heat and reactor vessel wall heat transfer is insufficient to account for the core dryout alone, and this further indicates that significant flow exited the reactor vessel through the cold legs (flow rate measurements are, unfortunately, difficult to interpret during this time period).

Reactor Vessel Energy Balance. The mass of liquid evaporated, ΔM, in the reactor vessel during a time interval Δt can be approximated by

$$\Delta M \cong \bar{q}\bar{A}\, h_{fg}\, \Delta t$$

where $\bar{q}$ and $\bar{A}$ are the time averaged heat fluxes and surface areas below the froth levels in the reactor vessel, and h_{fg} is the latent heat of evaporation. Saturated fluid conditions are assumed. The calculated mass evaporated between 120 and 190 s is 79 kg (175 lbm), while between 190 and 240 s, when the core dries out, it is 54 kg (120 lbm). The latter mass is a maximum value calculated by assuming that the heat transfer area extends to the core exit. The mass in the reactor vessel between the core entrance and exit at 190 s, assuming that $\bar{\alpha} = 0.5$, is ~261 kg (575 lbm). Therefore, during the 190- to 240-s interval, more mass exited the reactor vessel through the cold legs due to overflow of frothing downcomer fluid than by evaporation.

Entrainment Above Froth Level. There are no known accurate methods for calculating the small

entrainment rates of dispersed droplet flow above a boiling froth, so an order of magnitude approach is used. The following method is similar to that used by Banerjee[A-10] for the Experiment L5-1 TC response calculations.

Assuming no heat transfer above the midcore elevation, the vapor velocity, V_s, at one-half core uncovery is

$$V_s = \frac{0.5\ P_{core} + P_{RV\ into\ core}}{A_x \varrho_g h_{fg}}$$

$$= 1.11\ m/s = 3.64\ ft/s\ .$$

The terminal velocity, V_t, of drops and the maximum drop size, d, are given by

$$V_t = (\varrho_f - \varrho_g)\frac{d^2 g}{18\mu}\ ,$$

where V_t is in SI units and μ = viscosity.

$$V_t = 2.2 \times 10^6\ d^2 = 1.11\ m/s = 3.64\ ft/s\ .$$

The resultant drop diameter, d, is 7.1×10^{-4} m (2.3×10^{-3} ft).

To calculate the entrainment rate (the interfacial area formed for entrained drops per unit time), it was assumed that

1. Kinetic energy of vapor in a given control volume is used to form drops.

2. One-half percent of the total kinetic energy is used to form drops (Perry,[A-11] pp. 18-61, states that good atomizers use less than one percent of the available kinetic energy to increase the surface area of a fluid during drop formation).

Reference A-11 gives the relationship between the kinetic energy consumed and the resulting interfacial area formed:

$$a\sigma g = 0.005\left(0.5\varrho_g V_g^2 A_x V_g\right)$$

where

a = interfacial area formed/unit time

σ = surface tension

g = gravitational constant

$0.5\varrho_g V_g^2 A_x V_g$ = kinetic energy flow rate.

This relationship gives an entrainment rate proportional to V_g^3, which is empirically observed (see Reference A-11, pp. 18-65). For conditions at 190 s,

$$a = 3.82 \times 10^{-6}\ m^2/(s \cdot rod)$$

$$= 4.11 \times 10^{-5}\ ft^2/(s \cdot rod)\ .$$

Deposition Rate. Using the Whalley, et al., measurements reported in Reference A-12, deposition flux = $K_d C_E$

where

K_d = deposition coefficient ~ 0.1 m/s for a steam—water mixture

C_E = droplet concentration (kg/m^3)

$= (1 - \alpha)\ \varrho_f$

ϱ_f = saturated liquid density

$1 - \alpha$ = average flow area fraction of droplets.

The average flow area fraction of droplets, $1-\alpha$, assuming no evaporation and steady state flow, is given by

$$1 - \alpha = \frac{a}{4\pi r_d^2}\left(\frac{4}{3}\pi r_d^3\right)\left(\frac{1}{A_x V_g}\right) = 1.1 \times 10^{-5}$$

where

r_d = droplet radius.

For $\varrho_f = 942\ kg/m^3$,

$$K_d C_E = 0.1\ m/s \times 1.1 \times 10^{-5} \times 942\ kg/m^3$$

$$= 1.0 \times 10^{-3}\ kg/(m^2 \cdot s)$$

$$= 2.1 \times 10^{-4}\ lbm/(ft^2 \cdot s)$$

and

$$\text{deposition rate} = \text{flux}/\varrho_f = 1.1 \times 10^{-3} \text{ mm/s}$$

$$= 4.3 \times 10^{-5} \text{ in./s} .$$

The average flow area fraction obtained corresponds to a flow quality, x, of 0.992. The entrainment flux is therefore very small, and it is calculated from an energy balance that less than 1 K (1.8°F) superheating will evaporate the entrained drops. The evaporation and dry wall heat transfer will gradually decay steam superheating.

Therefore, the upper-plenum liquid that coats the TCs is not the result of entrainment, but is rather a remnant of the froth level extending into the upper plenum before 190 s. Depending on the core exit steam velocity, this liquid will either drain into the core, be held up in the upper plenum if the steam velocity is high enough for countercurrent flow limiting (CCFL) conditions, or be swept out the upper plenum by concurrent annular flow or entrainment if the steam velocity is very high, which, as we have seen, it is not. The remaining liquid in the upper plenum will not evaporate without significant superheated steam flow from the core and, since $dP/dt \cong 0$, there is no evaporation due to depressurization. Calculations of upper-plenum CCFL conditions are given in the following section.

Upper-Plenum Drainage and Flooding. Liquid in the upper plenum will drain back into the core unless steam velocity is high enough at the core exit or within the upper plenum to prevent it. Drainage is reduced or stopped by interphase drag at high steam velocities. The CCFL velocity is the critical velocity above which drainage is prevented. At less than the CCFL velocity, drainage will be slowed by steam flow but not stopped. The onset of the CCFL condition is not continuous, however, but corresponds to a sudden instability. The CCFL velocity is usually calculated using correlations such as that given by Wallis.[A-13] These correlations are inaccurate, however, outside their data ranges and for different system geometries. Fortunately, for our purposes, Jacoby and Mohr have studied CCFL in upper-plenum components at the INEL.[A-5] Also, steam—water flooding experiments for a BWR fuel bundle upper grid plate have been used to correlate CCFL conditions[A-6] with Kudateladze numbers for the gas and liquid phases (K_g and K_f):

$$K_g^{0.5} + AK_f^{0.5} = B$$

where

$$K_g = j_g \varrho_g^{0.5} [g_c \, g \, \sigma(\varrho_f - \varrho_g)]^{-0.25}$$

$$K_f = j_f \varrho_g^{0.5} [g_c \, g \, \sigma(\varrho_f - \varrho_g)]^{-0.25}$$

and

j = volumetric flux (gas or liquid)

ϱ = density (gas or liquid)

g_c = dimensional constant = 1 in SI units = 32.174 (lbm·ft)/(lbf·s^2)

g = gravitational constant

σ = surface tension

A, B = constants

f subscript denotes liquid

g subscript denotes gas.

A and B were taken from Reference A-5, for Westinghouse components. CCFL conditions will occur in the upper plenum when $K_g^{0.5} \cong B \geq 1.31$, the minimum value for a component in Reference A-5. Figure A-6 gives a typical curve for liquid carry-over as a function of the Kudateladze number and shows the onset of flooding.

The steam—water CCFL tests reported by Sun,[A-6] however, indicate that the minimum $K_g^{0.5}$ for upper grid plates for 7 x 7 and 8 x 8 PWR fuel assemblys are ~1.8 and ~2.08, respectively. Since this PWR grid plate geometry is similar to that in LOFT, these values are probably close to the LOFT value and 1.31 is probably low.

The maximum calculated $K_g^{0.5}$ for 190 to 380 s in the LOFT experiment is 0.95, for a location above the center fuel assembly—where power is maximum—and at the fuel assembly upper grid plate—where the flow area is less than the core flow area [(~0.09 m^2 (1.0 ft^2) compared with 0.16 m^2 (1.7 ft^2)]. This calculation indicates that complete

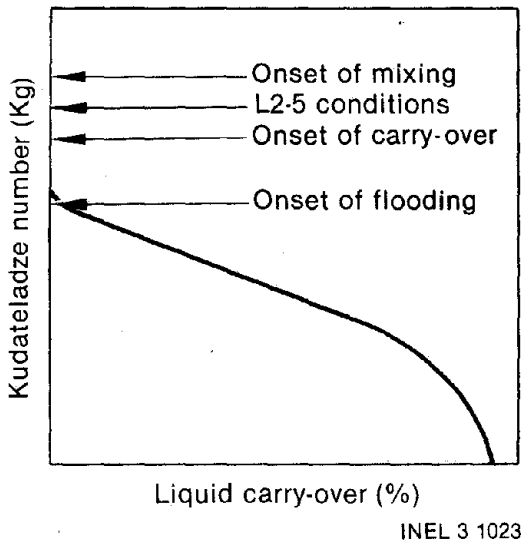

Figure A-6. Typical liquid carry-over as a function of Kudateladze number.

CCFL conditions are not obtained, but that drainage is reduced (the conclusion is the same when the Wallis correlation is used). These conditions for experiment L2-5 are also indicated on Figure A-6. This situation corresponds to what Lee, McCarthy, and Tien[A-14] refer to as the mixed countercurrent flow condition, shown in Figure A-7.

As shown in Figures A-8 and A-9, after low-pressure injection was reinitiated at 347 s, the steam velocity greatly increased due to rapid boiling associated with fuel rod quenching during reflood.

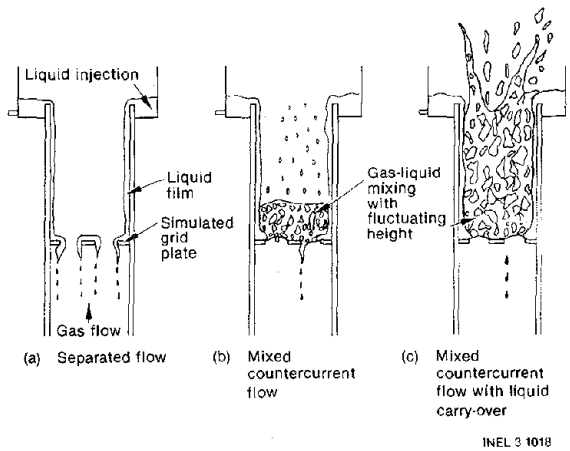

Figure A-7. Countercurrent flow configurations for simulated fuel bundle upper grid plate.

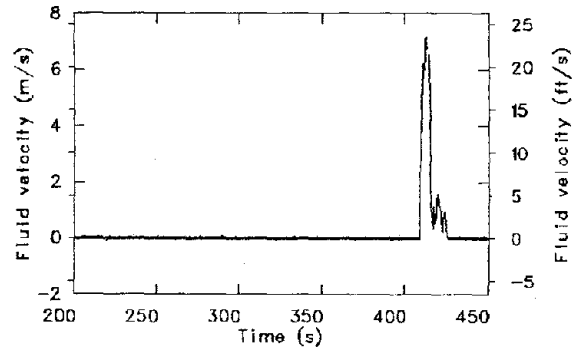

Figure A-8. Upper-plenum fluid velocity during the Experiment L2-5 second heatup.

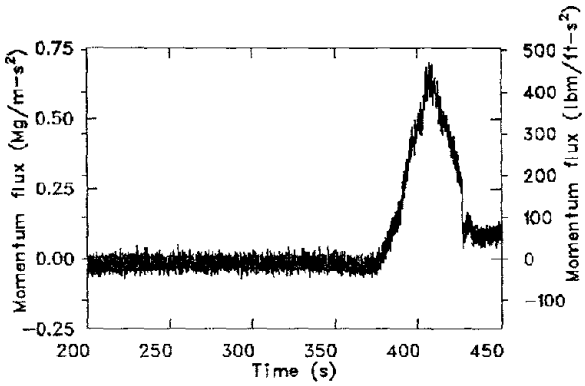

Figure A-9. Upper-plenum fluid momentum flux during the Experiment L2-5 second heatup.

Figure A-8 shows the increase in upper-plenum fluid velocity as measured by a turbine meter. This increase is corroborated by the measured fluid momentum flux shown in Figure A-9. The maximum measured upper-plenum velocity of ∿7 m/s (23 ft/s) corresponds to a $K_g^{0.5}$ of ∿1.4. Although this velocity is probably less than the CCFL velocity for the plate, it may be sufficient to strip liquid from the core exit TCs. Therefore, core exit TC dryout and subsequent heatup is judged to be due to both evaporation by superheated steam and to mechanical stripping of the liquid from the TCs.

Rod Top Quenching. The L2-5 data indicate that after the high steam velocities associated with low-pressure coolant injection began to subside at about 410 s, the cladding TCs at the 1.57-m (62-in.) elevation and the core exit TCs quenched; about 15 s later the cladding TCs at the 1.47-m (58-in.) elevation quenched (Figure A-10). This indicates a top-down quench to the 1.47-m (58-in.) elevation. The quench is bottom-up at elevations lower than about 1.37 m (54 in.). The top-down quench velocity of

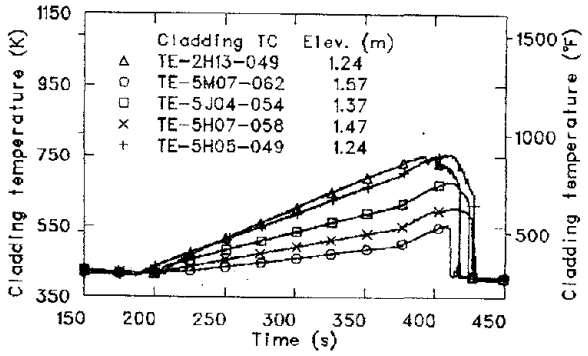

Figure A-10. Typical cladding temperatures, showing quenching behavior at different elevations during the Experiment L2-5 second heatup.

~0.8 cm/s (~0.3 in./s) corresponds reasonably well to a calculated value of 1.1 cm/s (0.43 in./s) using the Yamanouchi equation for falling film rewetting.[A-15] The reactor vessel wall temperature at the 1.47-m (58-in.) elevation and wall properties for Zircaloy-4 cladding[A-16] were used in this calculation of quench velocity.

The quench velocity calculation implies that, since there was no top-down quenching between 190 and 410 s, and since some drainage of upper-plenum fluid is predicted, there was only a small quantity of liquid in the upper plenum during this period. This small, but unknown, quantity of liquid was sufficient to keep the core exit TCs quenched until 380 s.

Conclusions

The results of the above calculations support the following secondary heatup scenario, which is shown schematically in Figure A-11.

1. When the low-pressure and high-pressure injection systems were terminated at 107 and 144 s, respectively, the core and upper plenum were filled with a bubbly froth that cooled the core (Figure A-11a). The core, however, was not liquid full, and the collapsed liquid level [1.2 m (47 in.)] was lower than the top of the core [1.68 m (66 in.)].

2. At 144 s and during the remainder of the heatup transient (until 400+ s), the lower plenum was full of two-phase froth generated by heat transfer from the reactor vessel. The calculated downcomer collapsed liquid level is close to that in the core. The froth spilled out the downcomer and into the intact- and broken-loop cold legs.

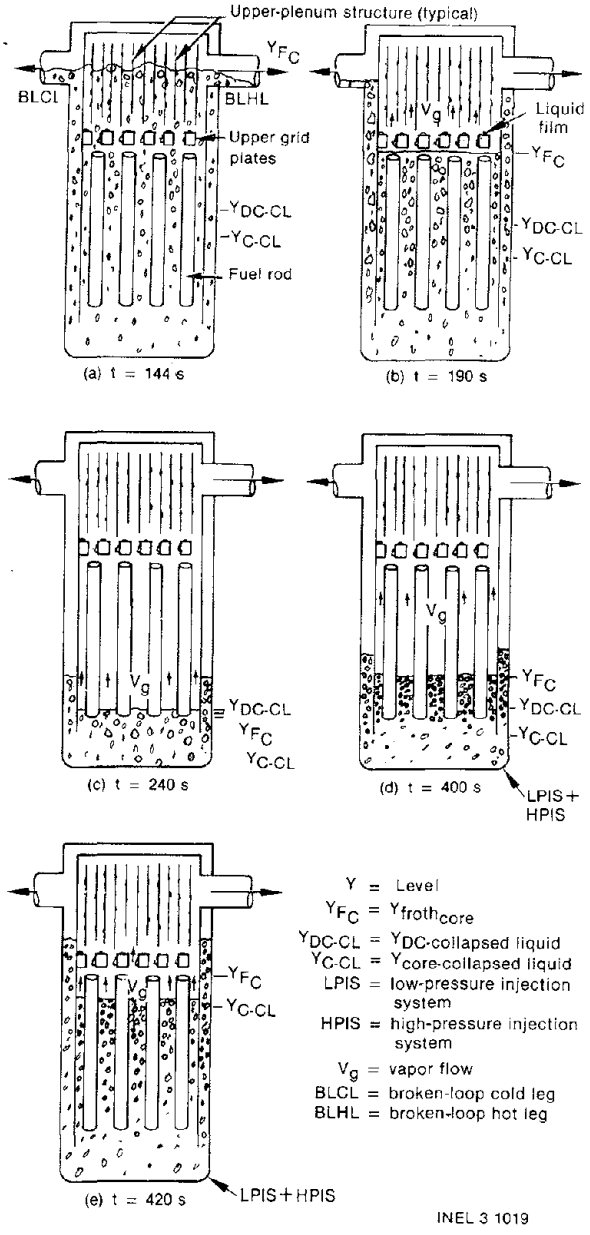

Figure A-11. Second heatup scenario for Experiment L2-5.

3. At 190 s into the transient, the collapsed liquid level in the core was at ~0.84 m (~33 in.) and the froth level was just at the core top (Figure A-11b). As the froth level decreased, the top-down core heatup was initiated. The rods heated at close to the adiabatic rate.

4. The mechanism for the departure from nucleate boiling and subsequent heatup was a dryout rather than a pool-boiling type CHF.

5. The liquid mass that had boiled off in the reactor vessel between 144 and 190 s was insufficient to completely void the upper plenum (Figure A-11b). The remaining mass flowed out the downcomer by froth spillover into the intact and broken cold legs. Subsequent to 190 s, mass continued to spill over into the downcomer, acting in concert with fluid boiloff to uncover the core.

6. Core exit TCs were covered by a film of draining liquid that remained after the froth level subsided (Figure A-11c). Steam velocity in the upper plenum was less than the CCFL velocity and was therefore insufficient to prevent drainage. The liquid film was sufficient to cool the TCs to saturation temperature until significant flow of superheated steam began to evaporate and sweep away the film at 370 s. The high steam flow was generated by reflood quenching of the core from the bottom up (Figure A-11d).

7. After the rods were quenched to above the 1.27-m (50-in.) elevation (three-fourths of the core height) at 415 s, the core power generated steam flow decreased and the top of the rods were quenched (Figure A-11e) by a falling film to approximately the 1.47-m (58-in.) elevation.

8. Because of wetting, the core exit TCs did not indicate inadequate core cooling to the reactor operators.

References

A-1. J. P. Adams, *Quick-Look Report on LOFT Nuclear Experiments L5-1 and L8-2*, EGG-LOFT-5625, October 1981.

A-2. D. B. Jarrell and J. M. Divine, *Experiment Data Report for LOFT Intermediate Break Experiment L5-1 and Severe Core Transient Experiment L8-2*, NUREG/CR-2398, EGG-2136, November 1981.

A-3. G. L. Shires, et al., "An Experimental Study of Level Swell in a Partially Water Filled Fuel Cluster," *Nuclear Energy, 19*, 5, October 1980.

A-4. A. Annunziato, M. Cumo, G. Palazzi, "Uncovered Core Heat Transfer and Thermal Non-Equilibrium," *Proceedings of 7th International Heat Transfer Conference, Munich 1982*, Washington, DC: Hemisphere Publishing, 1982.

A-5. J. K. Jacoby and C. M. Mohr, "Final Report on 3-D Experiment Project Air-Water Upper Plenum Experiment," 3DP-TR-001, EG&G Idaho, Inc. Idaho Falls, Idaho, November 1978.

A-6. K. H. Sun, "Flooding Correlations for BWR Bundle Upper Tieplates and Bottom Side-Entry Orifices," *Proceedings of the Second Multi-Phase Flow and Heat Transfer Symposium-Workshop, Miami Beach, April 1979.*

A-7. G. E. McCreery and P. E. Demmie, "Preliminary Analysis Results of Post L2-5 Core Heatup," in letter from L. P. Leach to R. E. Tiller, LPL-223-82, EG&G Idaho, Inc., Idaho Falls, Idaho, September 1982.

A-8. R. T. Lahey, Jr. and F. J. Moody, *The Thermal-Hydraulics of a Boiling Water Nuclear Reactor*, The American Nuclear Society, 1979.

A-9. K. H. Sun, R. B. Duffey, C. M. Peng, 'The Prediction of Two-Phase Mixture Level and Hydrodynamically-controlled Dryout Under Low FLow Conditions," *International Journal of Multi-Phase Flow, 7*, 5, 1981.

A-10. S. Banerjee, "L5-1 Thermocouples Response Calculations," in letter from G. E. McCreery to J. H. Linebarger, GEM-14-81, EG&G Idaho, Inc., Idaho Falls, Idaho, 1981.

A-11. R. H. Perry and C. H. Chilton (eds.), *Chemical Engineers' Handbook*, New York: McGraw-Hill Book Co., Inc., 1973.

A-12. P. B. Whalley and G. F. Hewitt, *The Correlation of Liquid Entrainment Fraction and Entrainment Rate in Annular Two Phase Flow*, AERE-R9187, UKAEA, Harwell, England, 1978; reported in *Handbook of Multi-Phase Systems*, G. Hetstroni (ed.), New York: McGraw-Hill Book Co., Inc., 1982, pp 2-71 to 2-73.

A-13. G. B. Wallis, *One-Dimensional Two-Phase Flow*, New York: McGraw-Hill Book Co., Inc., 1969.

A-14. H. M. Lee, G. E. McCarthy and C. L. Tien, *Liquid Carry-over and Entrainment in Air-Water Counter Current Flooding*, EPRI NP-2344, April 1982.

A-15. Yamanouchi, A., "Effect of Core Spray Cooling in Transient State After Loss-of-Coolant Accident," *Nuclear Applications, 5*, 1968.

A-16. D. L. Reeder, *LOFT System and Test Description*, NUREG/CR-0247, July 1978.